SOUTHWEST RESEARCH INSTITUTE
8500 Culebra Road, San Antonio, Texas 78228

TRANSMISSION CHARACTERISTICS OF CONICAL SHELLS UNDER LATERAL EXCITATIONS

by

Daniel D. Kana
William C. L. Hu

Final Report Part II
Contract NAS 5-10312
SwRI Project 02-2034

Prepared for

Goddard Space Flight Center
Greenbelt, Maryland

February 1968

Approved:

pr H. Norman Abramson, Director
Department of Mechanical Sciences

ABSTRACT

A theoretical and experimental study is presented for determining the steady-state frequency response of laterally excited truncated cones and cylinders in a low to moderate frequency range. The theoretical results are formulated in terms of forward transmission matrices, although relationships are reviewed which allow application of the results for impedance or admittance formulations as well. Expressions for the 4×4 matrices of transmission for coupled bending-shear displacements are developed by means of the membrane theory of thin shells. The results are then applied to the case of laterally excited shells which support a rigid top mass. Input and transfer pseudoimpedances are calculated and compared with experimental observations for 30° and 15° cones and a cylinder. Overall comparison of the results indicates that the membrane theory provides a reasonable approximation for determining response characteristics, but some definite deficiencies remain unexplained. A digital computer program is included for computing all required results.

TABLE OF CONTENTS

LIST OF ILLUSTRATIONS

LIST OF ILLUSTRATIONS (Cont'd)

NOMENCLATURE

a	major base radius of cone
$\bar{A}$, $\bar{B}$, $\bar{C}$, $\bar{D}$	submatrices of forward transmission matrix
b	minor base radius of cone
E	shell elastic modulus
$\bar{F}_1$, $\bar{F}_2$	generalized input and output force vectors, respectively
G	shell shear modulus
h	shell wall thickness
I	mass moment of inertia of supported mass about axis through center of mass
M	net moment on a cross section
N_s, N_θ, $N_{s\theta}$	membrane stress resultants
Q	net lateral shearing force on a cross section
s, θ	coordinates of point on cone surface (s is dimensional)
$s_1(1 - \gamma)$	slant length of truncated cone
u, v, w	local axial, tangential, and radial displacements of shell middle surface--these displacements lie parallel and perpendicular to the shell generating surface.
U, V, W	integrated axial, lateral, and radial displacements, respectively
U^*, V^*, W^*	net axial, lateral, and radial displacements, respectively
$\bar{V}_1$, $\bar{V}_2$	generalized input and output velocity vectors, respectively
x, θ	nondimensional coordinates of point cylinder surface
$(\dot{\ })$	denotes a velocity for indicated displacement
α	semivertex angle for cones

α_{ij}	elements of forward transmission matrix for velocities
β_{ij}	elements of forward transmission matrix for displacements
γ	geometric ratio for truncated cones
δ	offset of center of supported mass from plane including upper weld circle
Ψ	angular rotation of a cross section
ν	Poisson's ratio for shell
ξ	nondimensional cone coordinate $(\xi = \frac{s}{a} \sin \alpha)$
ρ	shell mass density
ϕ_{ij}, γ_{ij}	elements of conversion matrices
ω	circular frequency
Ω	nondimensional frequency parameter

INTRODUCTION

Within the last several years, steady-state frequency response methods have become increasingly popular for the description of dynamic behavior of linear mechanical systems. Impedance, admittance (mobility), and rearward and forward transmission methods all fall into this category of analysis. Basically, all these methods are similar in that they envision a mechanical component which possesses terminals that identify the position and direction of all external forces applied to the component and the corresponding velocities resulting from the application of those forces. The component is considered to be a "black box" whose character is determined in terms of the behavior at the accessible terminals. The methods can be applied to components that have either discrete or distributed properties, and complex systems can readily be synthesized into elements which can represent various structural, acoustical, electrical, etc., components.

Because of the nature of multi-degree of freedom and distributed components of complex systems, the above methods lend themselves immediately to matrix notation. Thus, a component can be described in terms of its impedance, admittance (mobility), or forward or rearward transmission matrix, whose elements are usually frequency dependent. The use of truncated conical or cylindrical shells as components of a complex structure such as a space vehicle falls into this category.

The purpose of the present research program has been to determine the frequency dependent matrices which describe truncated conical and cylindrical shells so that they can be used as components for the application of the above methods to the analysis of complex mechanical space vehicle systems. This has been achieved in terms of transmission matrices for axisymmetric modes in the first half of the program, and the results of this work have already been reported[1].

The second half of the present program has dealt with lateral bending responses of truncated cones and cylinders so that more complicated matrix representations result from the additional variables required to describe the complete response. The purpose of this report is to present the work accomplished under this final phase of the program. Again the characteristics of truncated conical and cylindrical shells have been developed in terms of transmission (specifically forward transmission) matrices. However, in order to facilitate using the results in analyses incorporating impedance or mobility methods, we begin with a discussion of the relationship between the various methods that have been mentioned. At the same time, a summary of the most recently accepted definitions utilized in the various methods is presented.

The approach used for the determination of the transmission matrices of truncated conical and cylindrical shells subject to lateral bending is similar to that used in the earlier work for longitudinal excitation[1]. Membrane theory of thin shells is used to derive expressions for the elements of a 4×4 transmission matrix. For the case of truncated cones, the governing equations must be integrated numerically, while, for the cylinder, the governing equations are integrated directly; but extensive numerical computations are still required to obtain the matrix elements. A computer program has been developed for this purpose and is included in the results. Experimental results from measurements of pseudoimpedances of several specimens are then compared with predicted results.

It should be mentioned that the present analysis is basically the same as that which has been reported in an earlier progress report[2]. However, the notation and arrangement of the analysis have been changed considerably so that they correspond with results and definitions reported in the recent work described in the next section.

RELATIONSHIPS BETWEEN IMPEDANCE, ADMITTANCE, AND TRANSMISSION MATRICES

Definitions of the various aspects of the several methods of response analysis, as well as the relationships between the matrices which characterize the components used for each method, have recently been described quite vividly by Rubin[3, 4]. For convenience, a brief review of these descriptions will be presented here; however, the referenced papers should be consulted for complete details. We emphasize that these relationships then allow conversion of the results to be presented for cones and cylinders from transmission to either impedance or admittance matrices. Although Rubin has described analyses which employ rectangular matrices[3], here we will consider only square matrices[4].

We introduce the notation:

$$\bar{F}_1 = \begin{Bmatrix} \mathcal{F}_{11} \\ \mathcal{F}_{12} \\ \vdots \\ \mathcal{F}_{1n} \end{Bmatrix}, \quad \bar{V}_1 = \begin{Bmatrix} v_{11} \\ v_{12} \\ \vdots \\ v_{1n} \end{Bmatrix} \tag{1}$$

as generalized force and velocity vectors, respectively, applied at the input to a "black box" component. The generalized forces $\mathcal{F}_{ij}$ can be forces, moments, etc., while the velocities v_{ij} can be translational, rotational, etc., velocities. Each is understood to represent a steady-state complex vector. Correspondingly, at the output terminals, we have

$$\bar{F}_2 = \begin{Bmatrix} \mathcal{F}_{21} \\ \mathcal{F}_{22} \\ \vdots \\ \mathcal{F}_{2n} \end{Bmatrix}, \quad \bar{V}_2 = \begin{Bmatrix} v_{21} \\ v_{22} \\ \vdots \\ v_{2n} \end{Bmatrix} \tag{2}$$

Now, with these definitions, the following partitioned matrix forms can be introduced:

$$\begin{Bmatrix} \bar{V}_1 \\ \bar{V}_2 \end{Bmatrix} = \begin{bmatrix} H & G \\ G^T & E \end{bmatrix} \begin{Bmatrix} \bar{F}_1 \\ \bar{F}_2 \end{Bmatrix} \quad \text{(Admittance)} \tag{3}$$

$$\begin{Bmatrix} \bar{F}_1 \\ \bar{F}_2 \end{Bmatrix} = \begin{bmatrix} S & R \\ R^T & Q \end{bmatrix} \begin{Bmatrix} \bar{V}_1 \\ \bar{V}_2 \end{Bmatrix} \quad \text{(Impedance)} \tag{4}$$

$$\begin{Bmatrix} \bar{F}_2 \\ \bar{V}_2 \end{Bmatrix} = \begin{bmatrix} A & B \\ C & D \end{bmatrix} \begin{Bmatrix} \bar{F}_1 \\ \bar{V}_1 \end{Bmatrix} \quad \text{(Rearward Transmission)} \tag{5}$$

$$\begin{Bmatrix} \bar{F}_1 \\ \\ \bar{V}_1 \end{Bmatrix} = \begin{bmatrix} \bar{A} & \bar{B} \\ \\ \bar{C} & \bar{D} \end{bmatrix} \begin{Bmatrix} \bar{F}_2 \\ \\ \bar{V}_2 \end{Bmatrix} \qquad \text{(Forward Transmission)} \qquad (6)$$

These forms are identical to Eqs. (20-23) of Reference 4, except for the bars on the notation of $\bar{F}_1$, $\bar{F}_2$, $\bar{V}_1$ and $\bar{V}_2$. For each case, the partitioned matrix in brackets represents an admittance, impedance, rearward transmission, or forward transmission matrix, respectively, all for the same "black box" component. We note one caution in the use of the forms. The force $\bar{F}_2$ used in the transmission matrices is the negative of the $\bar{F}_2$ in the admittance and impedance forms. For transmission matrices, $\bar{F}_2$ is the force applied by the output terminal 2 of the "black box," while, for admittance and impedance matrices, $\bar{F}_2$ is the force applied to terminal 2 of the "black box."

The relationships between the various forms above are shown in Figure 1 which has been taken directly from Reference 4. Row 1) shows the transformation from the admittance matrix to the other three forms. Similarly, rows 2), 3), and 4) show transformations beginning with the forward transmission, rearward transmission, and impedance matrices, respectively. All matrices on the indicated rows are square and have order n. The great utility of the transformations in Figure 1 becomes immediately obvious. The characteristic matrix of any component can be determined in terms of the form which is the most convenient, but can then be transformed to any of the other formulations.

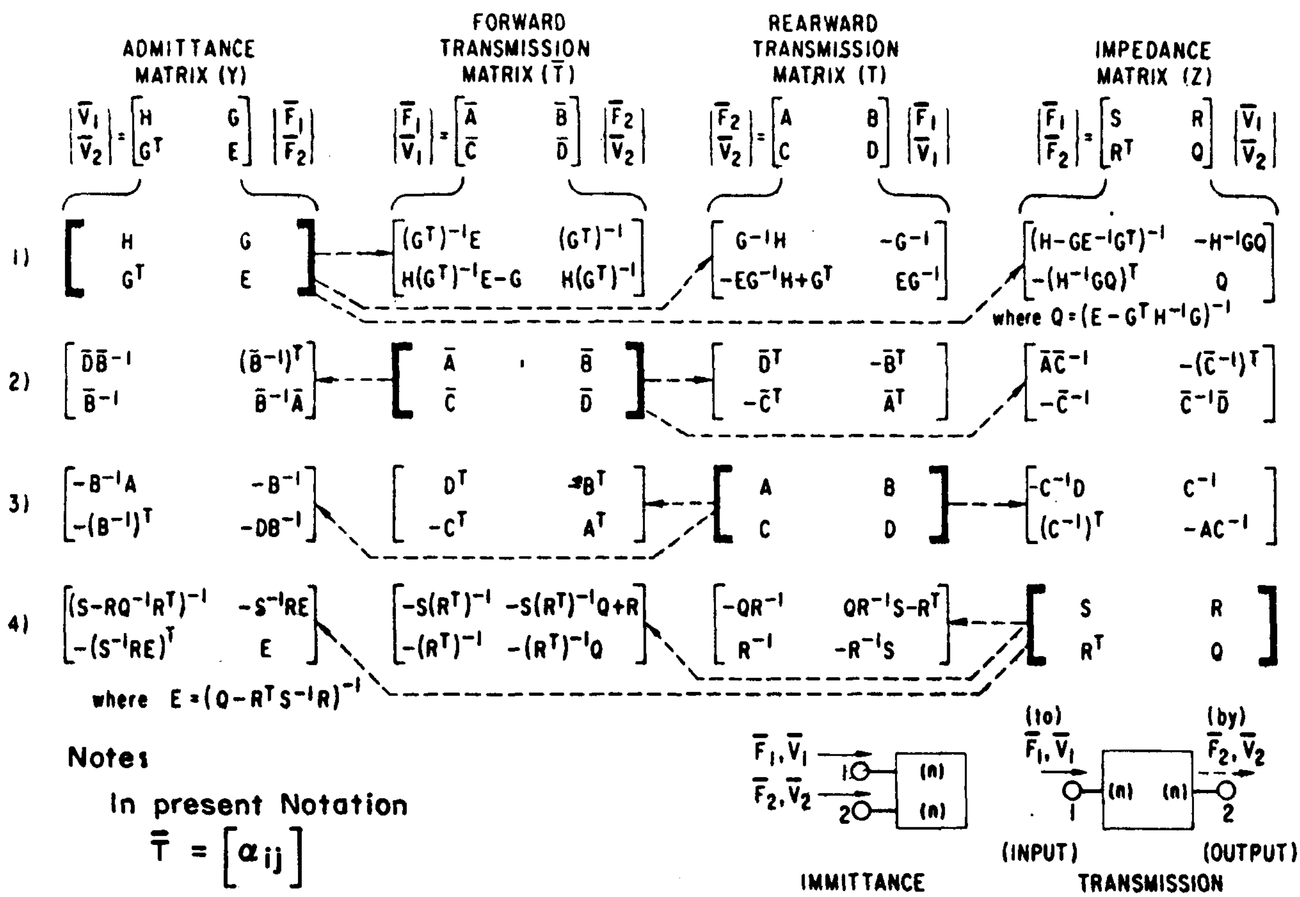

Figure 1. Relationships Among Admittance, Transmission, And Impedance Matrices

Mechanical impedance and admittance methods have been utilized for a longer period of time than the others, and, as a result, more literature is available on these methods. Reference lists of much of this literature are given in early reports of the present program[1, 2]. A very lucid description of applying mechanical impedance and admittance methods has been given by O'Hara[5]. He is particularly careful in pointing out the proper methods that must be utilized in measuring impedances and mobilities, which are the various elements of the impedance and admittance matrices, respectively. Diagonal elements are referred to as driving point, direct, or self-impedances or admittances, while off-diagonal elements are called transfer, cross, or mutual impedances or admittances. He further defines pseudoimpedance as the ratio of force input at some point of a structure to the velocity at some point. If the points are the same, driving point pseudoimpedance results, while, if the points are different, a transfer pseudoimpedance results.*

Additional recent examples of applying the impedance method in complex structures have been reported by On[6], while Rubin[3, 4] has described the use of all of the above methods. Rubin emphasizes the utility of the transmission matrix methods whereby the transmission matrix of a complex structure is formulated simply by multiplying in tandem all the matrices of the individual components--a procedure which is well suited to digital computation. Thus, the results of the present work,

---

*Note that with this definition, driving point and transfer pseudoimpedances were determined for cones and cylinders under longitudinal excitation in our earlier work, rather than driving point and transfer impedances as was indicated.

which are formulated in terms of forward transmission matrices, can be transformed to whatever method may be preferred, while the details of applying these methods to complex structures may be obtained from the references cited.

FORWARD TRANSMISSION MATRICES FOR COUPLED BENDING-SHEAR VIBRATIONS OF TRUNCATED CONICAL SHELLS

General Discussion

During the lateral vibration of a beam-type structural element, there will be, in general, a bending moment and a shearing force transmitted through each cross section, and the element will exhibit a coupled bending and shearing deformation. Due to this coupling, the structural element cannot be adequately described by a set of four-pole parameters as in the simpler case of longitudinal or torsional vibrations of the element[1]. In general, for lateral vibrations of a linear, elastic, beam-type element, there are four boundary force or velocity variables at each terminal. These quantities are transmitted through the structural element by a linear matrix equation:

$$\begin{Bmatrix} Q_1 \\ M_1 \\ \dot{V}_1 \\ \dot{\Psi}_1 \end{Bmatrix} = [a_{ij}] \begin{Bmatrix} Q_2 \\ M_2 \\ \dot{V}_2 \\ \dot{\Psi}_2 \end{Bmatrix} \qquad i, j = 1, 2, 3, 4 \tag{7}$$

where $\dot{V}$ denotes the lateral velocity of a cross section, $\dot{\Psi}$ the angular velocity, M the bending moment, and Q the shearing force; the subscript 1 refers to the input terminal, and the subscript 2 refers to the output terminal (Fig. 2).

The 4×4 matrix $[a_{ij}]$ is the forward transmission matrix of the structural component. Note from Eq. (6) that

$$\overline{F}_1 = \begin{Bmatrix} Q_1 \\ M_1 \end{Bmatrix} , \quad \overline{V}_1 = \begin{Bmatrix} \dot{V}_1 \\ \dot{\Psi}_1 \end{Bmatrix}$$

$$\overline{F}_2 = \begin{Bmatrix} Q_2 \\ M_2 \end{Bmatrix} , \quad \overline{V}_2 = \begin{Bmatrix} \dot{V}_2 \\ \dot{\Psi}_2 \end{Bmatrix}$$

It may also be noted that in Figure 2, for convenience, the sign convention on $\overline{F}_2$ is taken as positive generalized forces for Q_2 and M_2 applied to the output terminal 2 by the load. The sixteen elements a_{ij}, i, j = 1, 2, 3, 4, are, in general, frequency-dependent complex quantities, but are not all independent from each other[4]. In this case, it can be found that only ten of the sixteen elements are independent.

Derivations of Transmission Matrices for Truncated Conical Shells

We shall assume that for thin conical shells having a small semi-vertex angle α and an input frequency below a certain limiting value, the beam vibrations may be satisfactorily governed by the membrane theory of shells. Thus, referring to Figure 2 for the coordinate system, there are three equations of motion:

$$\frac{\partial N_s}{\partial s} + \frac{N_s}{s} + \frac{1}{s \sin\alpha} \frac{\partial N_{s\theta}}{\partial \theta} - \frac{N_\theta}{s} = \rho h \frac{\partial^2 u}{\partial t^2} \tag{8a}$$

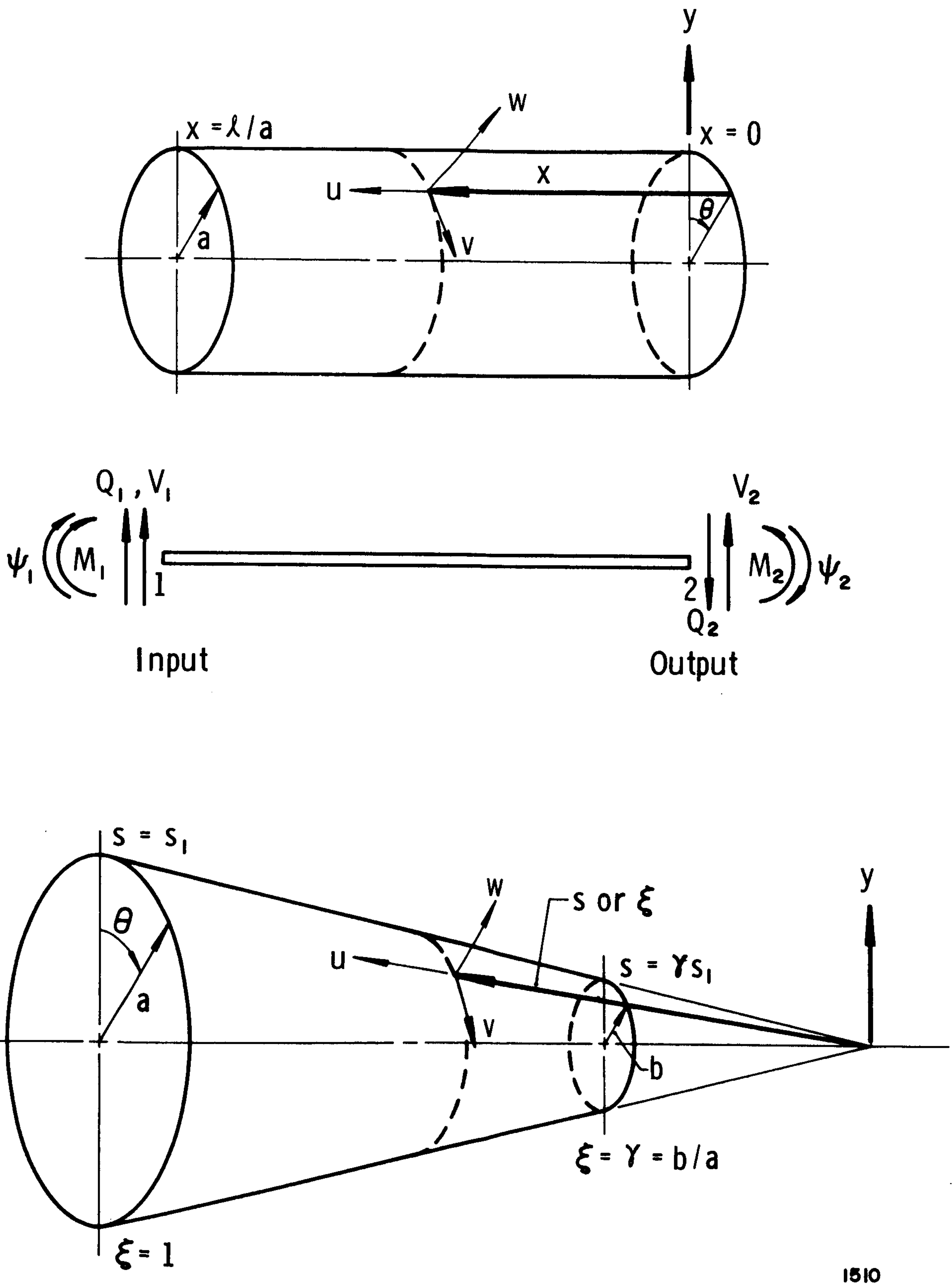

Figure 2. Coordinate System

$$\frac{\partial N_{s\theta}}{\partial s} + \frac{2}{s} N_{s\theta} + \frac{1}{s \sin\alpha} \frac{\partial N_\theta}{\partial \theta} = \rho h \frac{\partial^2 v}{\partial t^2} \tag{8b}$$

$$- \frac{1}{s \tan\alpha} N_\theta = \rho h \frac{\partial^2 w}{\partial t^2} \tag{8c}$$

and three stress resultant-displacement relations:

$$N_s = \frac{Eh}{1-\nu^2} \left[\frac{\partial u}{\partial s} + \nu \left(\frac{1}{s \sin\alpha} \frac{\partial v}{\partial \theta} + \frac{u}{s} + \frac{w}{s \tan\alpha} \right) \right] \tag{9a}$$

$$N_\theta = \frac{Eh}{1-\nu^2} \left[\frac{1}{s \sin\alpha} \frac{\partial v}{\partial \theta} + \frac{u}{s} + \frac{w}{s \tan\alpha} + \nu \frac{\partial u}{\partial s} \right] \tag{9b}$$

$$N_{s\theta} = \frac{Eh}{2(1+\nu)} \left[\frac{\partial v}{\partial s} + \frac{1}{s \sin\alpha} \frac{\partial u}{\partial \theta} - \frac{v}{s} \right] \tag{9c}$$

For lateral beam vibrations, we are interested in the following integrated quantities:

$$M = -s^2 \sin^2\alpha \cos\alpha \int_0^{2\pi} N_s \cos\theta \, d\theta \tag{10a}$$

$$Q = -s \sin\alpha \int_0^{2\pi} N_{s\theta} \sin\theta \, d\theta + s \sin^2\alpha \int_0^{2\pi} N_s \cos\theta \, d\theta \tag{10b}$$

along with

$$U = -\frac{1}{\pi} \int_0^{2\pi} u \cos\alpha \cos\theta \, d\theta \tag{11a}$$

$$V = -\frac{1}{\pi} \int_0^{2\pi} v \sin\theta \, d\theta \tag{11b}$$

$$W = -\frac{1}{\pi} \int_0^{2\pi} w \cos\alpha \cos\theta \, d\theta \tag{11c}$$

These definitions were originally given for a cylindrical shell by Simmonds[7], and the directions correspond to those for the input end in Figure 2. Equations (10) are a generalization of Simmonds' definitions to the case of a cone, while the displacement components given by Eqs. (11) have been defined here to allow maximum simplicity in the governing equations for the cone. It should be noted that the <u>net</u> displacements are given by

$$U^* = U - W \tan\alpha \tag{12a}$$

$$V^* = V \tag{12b}$$

$$W^* = W + U \tan\alpha \tag{12c}$$

where Eq. (12b) follows directly from Simmonds' definitions and applies as well for the case of a cone. The net rotation Ψ of a cross section will be introduced only later, for the resulting equations, which must be integrated numerically, are simpler in form when the variables (11) are utilized.

The governing equations will now be written in terms of the preceding definitions. We eliminate N_θ from Eqs. (8a), (8b), and (9b) by using Eq. (8c) and assuming harmonic oscillations in time. Then, by multiplying Eqs. (8a), (9a), (9b) by $\cos\theta$ and Eqs. (8b), (9c) by $\sin\theta$ and integrating over the circumference $\theta = 0$ to 2π (note that θ-derivative terms must be integrated by parts), we obtain the following equations governing the lateral beam vibrations of conical shells:

$$\frac{dM}{ds} = \pi\rho h\omega^2 \sin^2\alpha (W \tan\alpha - U)\, s^2 - Q\cos\alpha \tag{13a}$$

$$\frac{dQ}{ds} = \pi\rho h\omega^2 s \sin\alpha \,(W + U\tan\alpha - V) \tag{13b}$$

$$\frac{dU}{ds} = \frac{1}{\pi E h \sin^2\alpha}\frac{M}{s^2} - \frac{\nu\rho\omega^2 s \sin\alpha}{E\cos\alpha} W \tag{13c}$$

$$\frac{dV}{ds} = \frac{V}{s} + \frac{1}{\sin\alpha\cos\alpha}\frac{U}{s} + \frac{1}{\pi G h \sin\alpha\cos\alpha}\frac{M}{s^2} + \frac{1}{\pi G h \sin\alpha}\frac{Q}{s} \tag{13d}$$

$$W = -\left(1 - \frac{\rho\omega^2 s^2 \sin^2\alpha}{E\cos^2\alpha}\right)^{-1}\left[V + U\tan\alpha + \frac{\nu}{\pi E h \sin\alpha\cos\alpha}\frac{M}{s}\right] \tag{13e}$$

For convenience, we now introduce the dimensionless meridional coordinate

$$\xi = \frac{s}{s_1} = \frac{s}{a}\sin\alpha$$

where

$$\gamma \leq \xi \leq 1$$

and the dimensionless frequency parameter

$$\Omega^2 = \rho\frac{a^2\omega^2}{E}$$

The governing equations become

$$\frac{dV}{d\xi} = \frac{1}{\xi\sin\alpha}\left[V\sin\alpha + \frac{U}{\cos\alpha} + \frac{Q}{\pi G h} + \frac{\tan\alpha}{\pi G h a}\frac{M}{\xi}\right] \tag{14a}$$

$$\frac{dU}{d\xi} = \frac{1}{\sin\alpha}\left[\frac{M}{\pi E h a \xi^2} - \frac{\nu\Omega^2\xi}{\cos\alpha} W\right] \tag{14b}$$

$$\frac{dM}{d\xi} = \frac{\pi E h a \Omega^2 \xi^2}{\sin\alpha}(W\tan\alpha - U) - Qa\cot\alpha \tag{14c}$$

$$\frac{dQ}{d\xi} = \frac{\pi E h \Omega^2 \xi}{\sin\alpha} (W + U \tan\alpha - V) \tag{14d}$$

$$W = - \left(1 - \frac{\Omega^2}{\cos^2\alpha} \xi^2\right)^{-1} \left[V + U \tan\alpha + \frac{\nu}{\pi E h a \cos\alpha} \frac{M}{\xi}\right] \tag{14e}$$

This set of differential equations is in a convenient form for numerical integration. Note that the last equation is algebraic and serves to define the parametric function W.

Since the boundary conditions are usually prescribed on (Q, M, V, Ψ), we shall now derive a relation for the determination of the boundary values of U which appears in the differential Eqs. (14). The angle of rotation, Ψ, of an arbitrary cross section is defined as

$$\Psi = \frac{U^*}{a\xi} = \frac{U - W \tan\alpha}{a\xi} \tag{15}$$

Elimination of W from Eqs. (14e) and (15) gives

$$U = (1 - \Omega^2\xi^2)^{-1} \left[(\cos^2\alpha - \Omega^2\xi^2) a\xi\Psi - V \sin\alpha \cos\alpha - \frac{\nu \sin\alpha}{\pi E h a} \frac{M}{\xi}\right] \tag{16}$$

Now, four independent numerical integrations of Eqs. (14) for the four sets of initial values at $\xi = \gamma = b/a$,

$$\begin{aligned}
1)\quad & \{Q_2, M_2, V_2, \Psi_2\} &= \{1, 0, 0, 0\} \\
2)\quad & \{Q_2, M_2, V_2, \Psi_2\} &= \{0, 1, 0, 0\} \\
3)\quad & \{Q_2, M_2, V_2, \Psi_2\} &= \{0, 0, 1, 0\} \\
4)\quad & \{Q_2, M_2, V_2, \Psi_2\} &= \{0, 0, 0, 1\}
\end{aligned} \tag{17}$$

will yield the influence coefficients β_{ij} at the boundary $\xi = 1$:

$$\begin{aligned}
&1) \quad \{Q_1, M_1, V_1, \Psi_1\} &&= \{\beta_{11}, \beta_{21}, \beta_{31}, \beta_{41}\} \\
&2) \quad \{Q_1, M_1, V_1, \Psi_1\} &&= \{\beta_{12}, \beta_{22}, \beta_{32}, \beta_{42}\} \\
&3) \quad \{Q_1, M_1, V_1, \Psi_1\} &&= \{\beta_{13}, \beta_{23}, \beta_{33}, \beta_{43}\} \\
&4) \quad \{Q_1, M_1, V_1, \Psi_1\} &&= \{\beta_{14}, \beta_{24}, \beta_{34}, \beta_{44}\}
\end{aligned} \tag{18}$$

Note that the initial value U_2 at $\xi = \gamma$ should be calculated by substituting Eqs. (10) into Eq. (9):

$$\begin{aligned}
&1) \quad U_2 = 0 \\
&2) \quad U_2 = (1 - \Omega^2\gamma^2)^{-1} \left[- \frac{\nu \sin\alpha}{\pi E h a \gamma}\right] \\
&3) \quad U_2 = (1 - \Omega^2\gamma^2)^{-1} \left[- \sin\alpha \cos\alpha\right] \\
&4) \quad U_2 = (1 - \Omega^2\gamma^2)^{-1} \left[(\cos^2\alpha - \Omega^2\gamma^2)\, a\gamma\right]
\end{aligned} \tag{19}$$

The transmission matrix $[\beta_{ij}]$ now relates the boundary force and displacement variables as follows:

$$\begin{Bmatrix} Q_1 \\ M_1 \\ V_1 \\ \Psi_1 \end{Bmatrix} = [\beta_{ij}] \begin{Bmatrix} Q_2 \\ M_2 \\ V_2 \\ \Psi_2 \end{Bmatrix} \tag{20}$$

The conversion into $[a_{ij}]$ may be readily effected by using the relations

$$\dot{V} = i\omega V \quad , \quad \dot{\Psi} = i\omega\Psi$$

Thus, from Eqs. (6) and (7), we note that:

$$\left[\overline{A}\right] = \begin{bmatrix} \alpha_{11} & \alpha_{12} \\ \alpha_{21} & \alpha_{22} \end{bmatrix} = \begin{bmatrix} \beta_{11} & \beta_{12} \\ \beta_{21} & \beta_{22} \end{bmatrix}$$

$$\left[\overline{B}\right] = \begin{bmatrix} \alpha_{13} & \alpha_{14} \\ \alpha_{23} & \alpha_{24} \end{bmatrix} = \left(-\frac{i}{\omega}\right) \begin{bmatrix} \beta_{13} & \beta_{14} \\ \beta_{23} & \beta_{24} \end{bmatrix}$$

$$\left[\overline{C}\right] = \begin{bmatrix} \alpha_{31} & \alpha_{32} \\ \alpha_{41} & \alpha_{42} \end{bmatrix} = (i\omega) \begin{bmatrix} \beta_{31} & \beta_{32} \\ \beta_{41} & \beta_{42} \end{bmatrix} \tag{21}$$

$$\left[\overline{D}\right] = \begin{bmatrix} \alpha_{33} & \alpha_{34} \\ \alpha_{43} & \alpha_{44} \end{bmatrix} = \begin{bmatrix} \beta_{33} & \beta_{34} \\ \beta_{43} & \beta_{44} \end{bmatrix}$$

Special Case of Cylindrical Shell ($\alpha = 0$)

The governing equations for a cylindrical shell may be obtained directly from Eqs. (13) by letting

$$\alpha \rightarrow 0, \quad s \sin\alpha \rightarrow a, \quad \text{and} \quad \frac{d}{ds} \rightarrow \frac{d}{d\overline{x}} = \frac{1}{a}\frac{d}{dx} \quad \text{where } x = \frac{\overline{x}}{a}$$

We also note that

$$U \rightarrow U^*, \qquad V = V^*, \qquad \text{and} \qquad W \rightarrow W^*$$

so that we also have

$$\Psi = \frac{U^*}{a} = \frac{U}{a}$$

Thus, the equations become:

$$\frac{dM}{dx} = -\pi E h \Omega^2 a^2 \Psi - Qa \tag{22a}$$

$$\frac{dQ}{dx} = \pi E h \Omega^2 (W - V) \tag{22b}$$

$$\frac{d\Psi}{dx} = \frac{M}{\pi E h a^2} - \nu \frac{\Omega^2}{a} W \tag{22c}$$

$$\frac{dV}{dx} = a\Psi + \frac{Q}{\pi G h} \tag{22d}$$

$$W = -(1 - \Omega^2)^{-1} \left[V + \frac{\nu M}{\pi E h a} \right] \tag{22e}$$

Equations (22) are identical to Eqs. (30) thru (34) of Simmonds[7]. By eliminating M and Q from these equations, we obtain:

$$a \frac{\partial^2 \Psi}{\partial x^2} + \nu \left(\frac{\partial V}{\partial x} + \frac{\partial W}{\partial x} \right) + \frac{1 - \nu}{2} \left(\frac{\partial V}{\partial x} - a\Psi \right) + (1 - \nu^2)\, \Omega^2 a \Psi = 0$$

$$\frac{\partial^2 V}{\partial x^2} - a \frac{\partial \Psi}{\partial x} - 2(1 + \nu)\, \Omega^2 (W - V) = 0 \tag{23}$$

$$(1 - \nu^2)\Omega^2 W - \nu a \frac{\partial \Psi}{\partial x} - V - W = 0$$

which can be written as:

$$\begin{bmatrix} \mathcal{D}^2 - \frac{1-\nu}{2} + (1 - \nu^2)\Omega^2 & \frac{1+\nu}{2}\mathcal{D} & \nu\mathcal{D} \\ -\mathcal{D} & \mathcal{D}^2 + 2(1+\nu)\Omega^2 & -2(1+\nu)\Omega^2 \\ \nu\mathcal{D} & 1 & 1 - (1 - \nu^2)\Omega^2 \end{bmatrix} \begin{Bmatrix} a\Psi \\ V \\ W \end{Bmatrix} = 0$$

where $\mathcal{D} = d/dx$. By assuming solutions of the form $e^{\lambda x}$, we obtain the characteristic equation

$$\lambda^4 + 2P\lambda^2 - K = 0$$

$$P = \frac{\Omega^2}{2(1-\Omega^2)}\,[5 + 2\nu - (1+\nu)(3-\nu)\Omega^2]$$

$$K = \frac{\Omega^2}{(1-\Omega^2)}\,[1 - 2(1+\nu)\,\Omega^2]\,[2 - (1-\nu^2)\,\Omega^2]$$

whose solutions are

$$(i\lambda_1)^2 = -P - \sqrt{P^2 + K}$$
$$\lambda_2^2 = -P + \sqrt{P^2 + K}\quad ,\ \text{for}\quad P, K > 0 \tag{24}$$

The case of $P, K < 0$ will be discussed later.

The general solution to Eqs. (23), which corresponds to Eqs. (24), is

$$V = A_1 \cos\lambda_1 x + B_1 \sin\lambda_1 x + C_1 \cosh\lambda_2 x + D_1 \sinh\lambda_2 x$$

Upon substitution of this result into Eqs. (23), we find additionally

$$W = A_1 f_1 \cos\lambda_1 x + B_1 f_1 \sin\lambda_1 x + C_1 f_2 \cosh\lambda_2 x + D_1 f_2 \sinh\lambda_2 x$$

$$a\Psi = A_1 g_1 \sin\lambda_1 x - B_1 g_1 \cos\lambda_1 x + C_1 g_2 \sinh\lambda_2 x + D_1 g_2 \cosh\lambda_2 x$$

where

$$f_1 = \frac{\nu\lambda_1^2 - 1 - 2\nu(1+\nu)\Omega^2}{1 - (1+\nu)^2\Omega^2}\quad ,\quad f_2 = \frac{-\nu\lambda_2^2 - 1 - 2\nu(1+\nu)\Omega^2}{1 - (1+\nu)^2\Omega^2}$$

$$g_1 = \frac{(1-\nu^2)\Omega^2 f_1 - f_1 - 1}{\nu\lambda_1}\quad ,\quad g_2 = \frac{(1-\nu^2)\Omega^2 f_2 - f_2 - 1}{\nu\lambda_2}$$

and upon substitution of these expressions into Eqs. (22c, d), we obtain:

$$M = \frac{\pi a E h}{1-\nu^2}\,[(g_1\lambda_1 + \nu + \nu f_1)(A_1 \cos\lambda_1 x + B_1 \sin\lambda_1 x)$$
$$+ (g_2\lambda_2 + \nu + \nu f_2)(C_1 \cosh\lambda_2 x + D_1 \sinh\lambda_2 x)]$$

$$Q = \pi Gh\ [(\lambda_1 + g_1)(B_1 \cos \lambda_1 x - A_1 \sin \lambda_1 x) + (\lambda_2 - g_2)(C_1 \sinh \lambda_2 x + D_1 \cosh \lambda_2 x)]$$

Thus, all variables have now been determined in terms of the constants A_1, B_1, C_1, and D_1, which must be determined from the boundary conditions. If we let

$$\mu_1 = (g_1\lambda_1 + \nu + \nu f_1)\frac{\pi aEh}{(1-\nu^2)} \quad , \quad \mu_2 = (g_2\lambda_2 + \nu + \nu f_2)\frac{\pi aEh}{(1-\nu^2)}$$

$$\mu_3 = \pi Gh(\lambda_1 + g_1) \quad , \quad \mu_4 = \pi Gh(\lambda_2 - g_2)$$

$$\Lambda_1 = \frac{\lambda_1 \ell}{a} \quad , \quad \Lambda_2 = \frac{\lambda_2 \ell}{a}$$

then at $x = 0$, we have

$$\begin{Bmatrix} Q_2 \\ M_2 \\ V_2 \\ \Psi_2 \end{Bmatrix} = \begin{bmatrix} 0 & \mu_3 & 0 & \mu_4 \\ \mu_1 & 0 & \mu_2 & 0 \\ 1 & 0 & 1 & 0 \\ 0 & -\frac{g_1}{a} & 0 & \frac{g_2}{a} \end{bmatrix} \begin{Bmatrix} A_1 \\ B_1 \\ C_1 \\ D_1 \end{Bmatrix} = [\phi_{ij}] \begin{Bmatrix} A_1 \\ B_1 \\ C_1 \\ D_1 \end{Bmatrix} \tag{25}$$

and at $x = \ell / a$

$$\begin{Bmatrix} Q_1 \\ M_1 \\ V_1 \\ \Psi_1 \end{Bmatrix} = \begin{bmatrix} -\mu_3 \sin \Lambda_1 & \mu_3 \cos \Lambda_1 & \mu_4 \sinh \Lambda_2 & \mu_4 \cosh \Lambda_2 \\ \mu_1 \cos \Lambda_1 & \mu_1 \sin \Lambda_1 & \mu_2 \cosh \Lambda_2 & \mu_2 \sinh \Lambda_2 \\ \cos \Lambda_1 & \sin \Lambda_1 & \cosh \Lambda_2 & \sinh \Lambda_2 \\ \frac{g_1}{a} \sin \Lambda_1 & -\frac{g_1}{a} \cos \Lambda_1 & \frac{g_2}{a} \sinh \Lambda_2 & \frac{g_2}{a} \cosh \Lambda_2 \end{bmatrix} \begin{Bmatrix} A_1 \\ B_1 \\ C_1 \\ D_1 \end{Bmatrix} = [\gamma_{ij}] \begin{Bmatrix} A_1 \\ B_1 \\ C_1 \\ D_1 \end{Bmatrix} \tag{26}$$

Then, from Eqs. (20), (25) and (26), we may form the matrix equation

$$[\beta_{ij}] = [\gamma_{ij}]\,[\phi_{ij}]^{-1} \tag{27}$$

and the α_{ij} are again found as in Eq. (21).

We now return to Eqs. (24) for the case

$$\begin{aligned} (i\lambda_1)^2 &= -P - \sqrt{P^2 + K} \\ (i\lambda_2)^2 &= -P + \sqrt{P^2 + K} \end{aligned} \qquad \text{for } P > 0,\ K < 0,\ \sqrt{P^2 + K} \geq 0 \tag{28}$$

It can be seen that the form of the solution will change for this case, as well as other possible combinations of P and K, whose values are functions of frequency. Here, we will consider only the additional case of Eqs. (28) which occurs at the lowest frequency change corresponding to

$$\Omega^2 = \frac{1}{2(1+\nu)}$$

For the case of Eqs. (28), we have

$$V = A_2 \cos \lambda_1 x + B_2 \sin \lambda_1 x + C_2 \cos \lambda_2 x + D_2 \sin \lambda_2 x$$

and, upon substitution into Eqs. (23), we find

$$\begin{aligned} W &= A_2 f_1 \cos \lambda_1 x + B_2 f_1 \sin \lambda_1 x + C_2 f_2 \cos \lambda_2 x + D_2 f_2 \sin \lambda_2 x \\ a\Psi &= A_2 g_1 \sin \lambda_1 x - B_2 g_1 \cos \lambda_1 x + C_2 g_2 \sin \lambda_2 x - D_2 g_2 \cos \lambda_2 x \end{aligned}$$

where f_1, g_1, and g_2 are given as before, but

$$f_2 = \frac{\nu\lambda_2^2 - 1 - 2\nu(1+\nu)\Omega^2}{1 - (1+\nu)^2\Omega^2}$$

and, similar to before, we have

$$M = \frac{\pi a E h}{1 - \nu^2} \left[(g_1\lambda_1 + \nu + \nu f_1)(A_2 \cos \lambda_1 x + B_2 \sin \lambda_1 x)\right.$$

$$\left. + (g_2\lambda_2 + \nu + \nu f_2)(C_2 \cos \lambda_2 x + D_2 \sin \lambda_2 x)\right]$$

$$Q = \pi G h \left[(\lambda_1 + g_1)(B_2 \cos \lambda_1 x - A_2 \sin \lambda_1 x) + (\lambda_2 + g_2)(D_2 \cos \lambda_2 x - C_2 \sin \lambda_2 x)\right]$$

Finally, for this case, it can be seen that at $x = 0$:

$$[\phi_{ij}] = \begin{bmatrix} 0 & \mu_3 & 0 & \mu_5 \\ \mu_1 & 0 & \mu_2 & 0 \\ 1 & 0 & 1 & 0 \\ 0 & -\frac{g_1}{a} & 0 & -\frac{g_2}{a} \end{bmatrix} \qquad (29)$$

where

$$\mu_5 = \pi G h(\lambda_2 + g_2)$$

and, at $x = \ell/a$,

$$[\gamma_{ij}] = \begin{bmatrix} -\mu_3 \sin \Lambda_1 & \mu_3 \cos \Lambda_1 & -\mu_5 \sin \Lambda_2 & \mu_5 \cos \Lambda_2 \\ \mu_1 \cos \Lambda_1 & \mu_1 \sin \Lambda_1 & \mu_2 \cos \Lambda_2 & \mu_2 \sin \Lambda_2 \\ \cos \Lambda_1 & \sin \Lambda_1 & \cos \Lambda_2 & \sin \Lambda_2 \\ \frac{g_1}{a} \sin \Lambda_1 & -\frac{g_1}{a} \cos \Lambda_1 & \frac{g_2}{a} \sin \Lambda_2 & -\frac{g_2}{a} \cos \Lambda_2 \end{bmatrix} \qquad (30)$$

Then, Eqs. (27) and (21) are used for determining the coefficients α_{ij} for this case.

APPLICATION TO SHELL WITH RIGID TOP MASS

For a shell element which supports a rigid top mass and is excited laterally in translation only at the base, we have

$$\Psi_1 = 0 \quad , \quad Q_2 = -\omega^2 M^* V_2 \quad , \quad M_2 + Q_2\delta = -\omega^2 I \Psi_2$$

where the notation is indicated in Figure 3. Combining the last two equations

$$\Psi_1 = 0 \quad , \quad Q_2 = -\omega^2 M^* V_2 \quad , \quad M_2 = \omega^2 M^* \delta V_2 - \omega^2 I \Psi_2$$

and, by substituting these into Eqs. (20), we have

$$\left\{\begin{array}{c} Q_1 \\ M_1 \\ \hline V_1 \\ 0 \end{array}\right\} = \left[\begin{array}{cc} (-\beta_{11}\omega^2 M^* + \beta_{12}\omega^2 M^*\delta + \beta_{13}) & (-\beta_{12}\omega^2 I + \beta_{14}) \\ (-\beta_{21}\omega^2 M^* + \beta_{22}\omega^2 M^*\delta + \beta_{23}) & (-\beta_{22}\omega^2 I + \beta_{24}) \\ \hline (-\beta_{31}\omega^2 M^* + \beta_{32}\omega^2 M^*\delta + \beta_{33}) & (-\beta_{32}\omega^2 I + \beta_{34}) \\ (-\beta_{41}\omega^2 M^* + \beta_{42}\omega^2 M^*\delta + \beta_{43}) & (-\beta_{42}\omega^2 I + \beta_{44}) \end{array}\right] \left\{\begin{array}{c} V_2 \\ \Psi_2 \end{array}\right\}$$

$$= \left[\begin{array}{cc} c_{11} & c_{12} \\ c_{21} & c_{22} \\ \hline d_{11} & d_{12} \\ d_{21} & d_{22} \end{array}\right] \left\{\begin{array}{c} V_2 \\ \Psi_2 \end{array}\right\} \tag{31}$$

Partitioning the matrices as indicated, and dividing by V_1, we have

$$\left\{\begin{array}{c} Q_1/V_1 \\ M_1/V_1 \end{array}\right\} = [c_{ij}] \left\{\begin{array}{c} V_2/V_1 \\ \Psi_2/V_1 \end{array}\right\} \tag{32a}$$

$$\left\{\begin{array}{c} 1 \\ 0 \end{array}\right\} = [d_{ij}] \left\{\begin{array}{c} V_2/V_1 \\ \Psi_2/V_1 \end{array}\right\} \tag{32b}$$

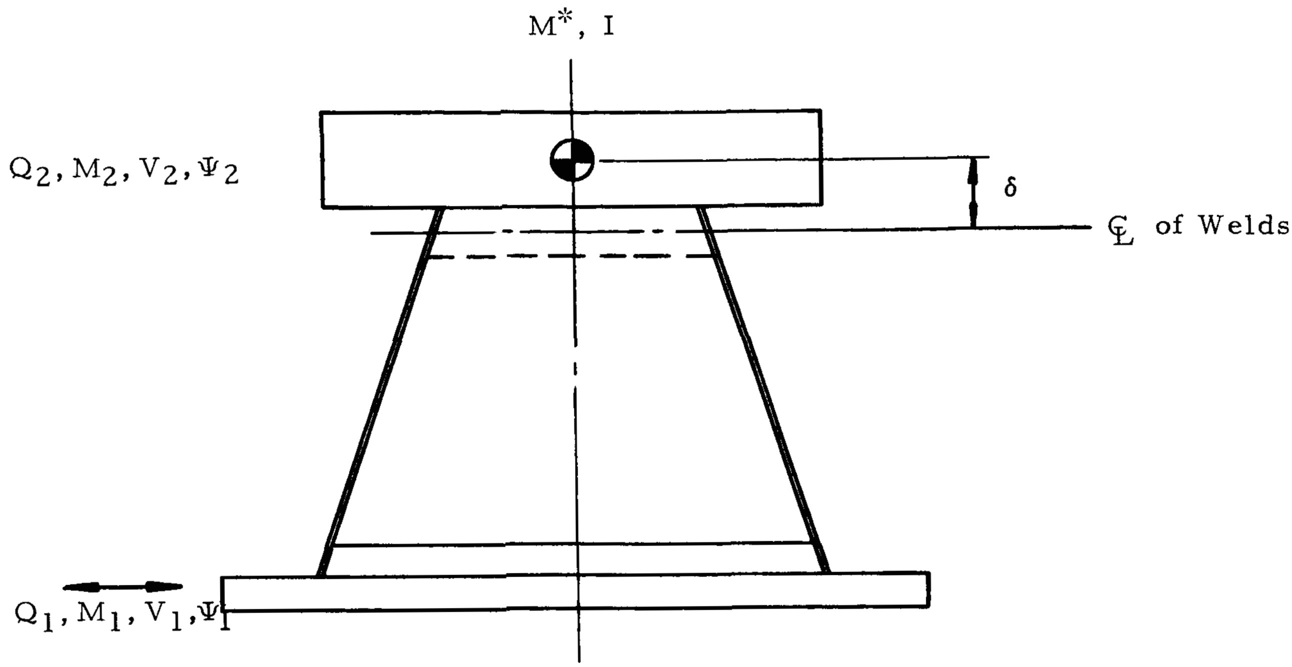

30° Cone (α = 30°)

a = 5 in., b = 2.5 in., $s_1(1-\gamma)$ = 5.00 in.

I = 0.519 lb in sec^2, δ = 1.08 in.

15° Cone (α = 15°)

a = 5 in., b = 2.5 in., $s_1(1-\gamma)$ = 9.66 in.

I = 0.519 lb in sec^2, δ = 1.08 in.

Cylinder (α = 0)

a = 5 in., ℓ = 15 in.

I = 0.547 lb in sec^2, δ = 0.56 in.

All Specimens

$M^*g = W_t$ = 32.8 lb.

h = 0.005 in., E = 30 x 10^6 psi

Figure 3. Schematic Of Rigid Top Mass On Shell

Now, from Eq. (32b), we have

$$\begin{Bmatrix} V_2/V_1 \\ \Psi_2/V_1 \end{Bmatrix} = [d_{ij}]^{-1} \begin{Bmatrix} 1 \\ 0 \end{Bmatrix} = \begin{Bmatrix} d_{22} \\ -d_{21} \end{Bmatrix} (d_{11}d_{22} - d_{12}d_{21})^{-1} \tag{33}$$

and recalling that

$$\dot{V} = i\omega V \quad , \quad \dot{\Psi} = i\omega\Psi$$

we have

$$(\dot{V}_2/\dot{V}_1) = (V_2/V_1) \tag{34a}$$

$$(\dot{\Psi}_2/\dot{V}_1) = (\Psi_2/V_1) \tag{34b}$$

along with

$$Q_1/\dot{V}_1 = -\frac{i}{\omega}[c_{11}V_2/V_1 + c_{12}\Psi_2/V_1] \tag{34c}$$

$$M_1/\dot{V}_1 = -\frac{i}{\omega}[c_{21}V_2/V_1 + c_{22}\Psi_2/V_1] \tag{34d}$$

$$Q_1/\dot{V}_2 = (Q_1/\dot{V}_1)(V_1/V_2) \tag{34e}$$

$$M_1/\dot{V}_2 = (M_1/\dot{V}_1)(V_1/V_2) \tag{34f}$$

Equations (34c, d) and (34e, f) express driving point and transfer pseudo-impedances, respectively. All of Eqs. (34) hold true for cylinders as well as for truncated cones.

EXPERIMENTAL APPARATUS AND PROCEDURE

The apparatus which has been designed to measure the behavior of cones under lateral excitation is basically the same as that used for longitudinal excitation in the earlier part of the program so that details of most of the apparatus can be obtained from the earlier report[1]. Only a brief description will be given here for those parts of the system which are different from that used for longitudinal excitation. A diagram of the apparatus is shown in Figure 4, while a photograph is shown in Figure 5.

The same two cones (15° and 30°) along with the same cylinder are used for the present tests under lateral excitation, and the same terminal weights (32.8 lb) are used at the output ends. However, the specimens are now excited laterally by the use of a horizontal slip table in conjunction with the electrodynamic shaker as shown in Figure 5. The same base rings and mounting plate are again utilized, except that an alteration in the force gage arrangement is necessary. As can be seen, two vertically oriented force gages are used for measuring input moment M_1, while two horizontally oriented force gages are used to measure input force Q_1. These horizontal force gages, one on each side of the base ring, have one end bolted to the lower base plate and one end bolted to the base ring on the cone. This design allowed for essentially no cross-signals between the force and moment gages. Input velocity and output velocity and rotation are measured by means of piezoelectric accelerometers. Thus, a bare minimum of additional apparatus was necessary over that required for the earlier studies incorporating longitudinal excitation.

The procedure for experimental measurement is essentially the same as that previously utilized. A similar mass-cancellation circuit is used for nullifying the force signal resulting from the base rings, and a frequency range of 20 to 600 cps is used.

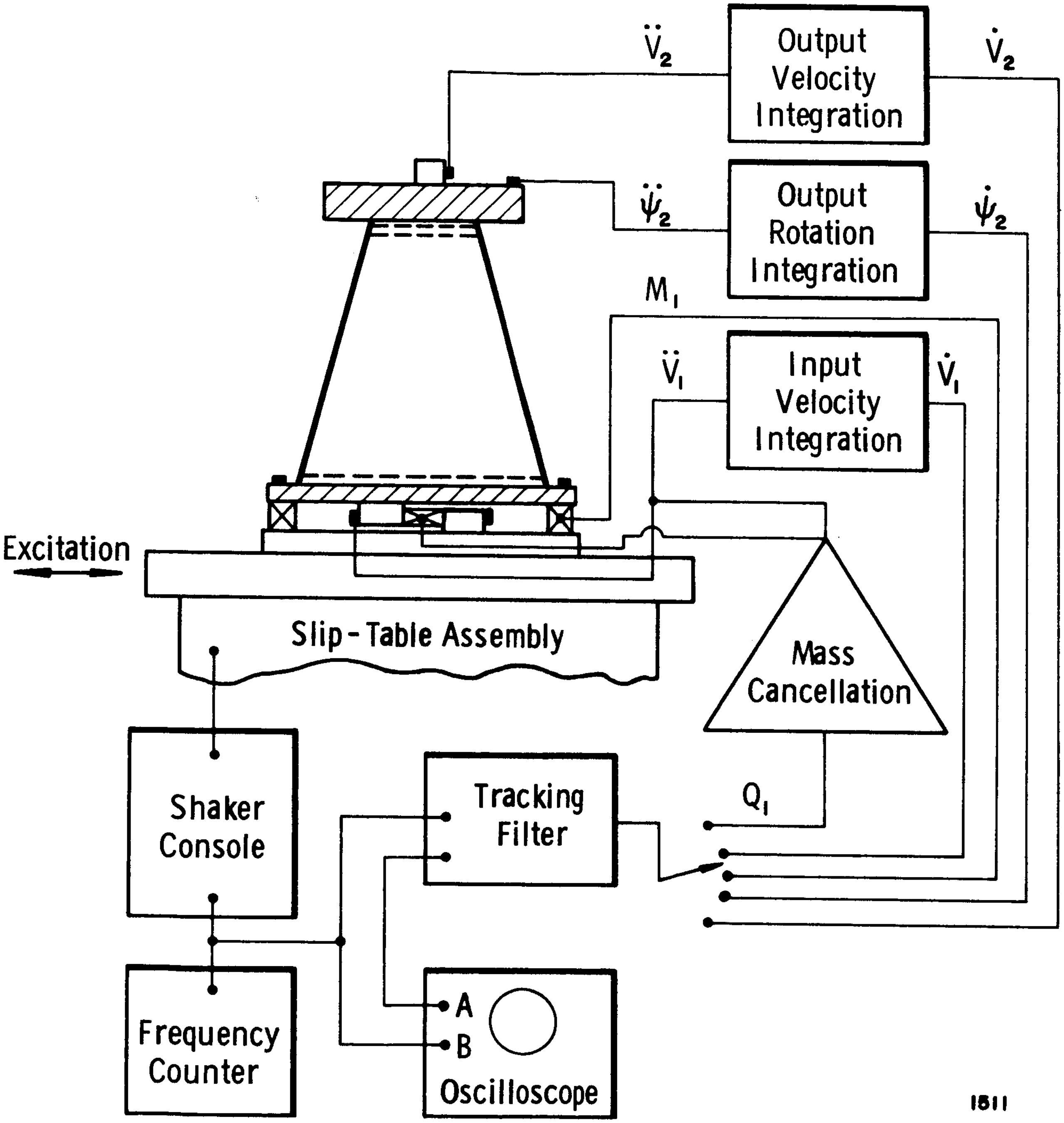

Figure 4. Diagram Of Experimental Apparatus

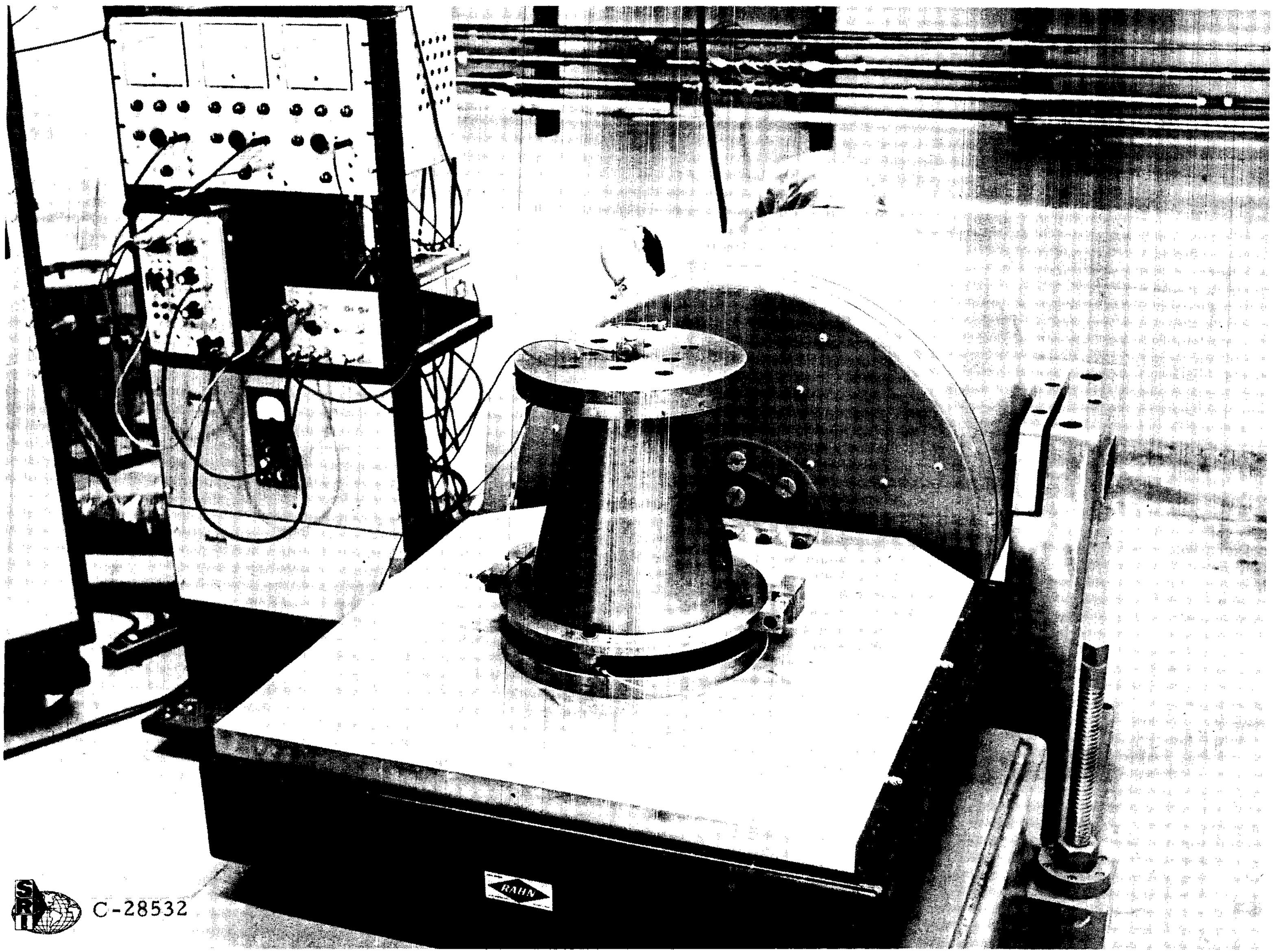

Figure 5. Apparatus For Lateral Pseudoimpedance Measurement With 15° Cone

RESULTS AND DISCUSSION

Theoretical and experimental results are presented in the remaining figures of this report. The results are presented in terms of the absolute values of the parameters indicated in Eqs. (34) for laterally excited specimens supporting a rigid top mass. Six different parameters were utilized in order to obtain a good overall picture of the dynamic behavior of the three specimens studied. The results, as presented in eighteen different figures, can conveniently be compared if they are laid out as indicated in Figure 6. This arrangement allows a quick comparison among the six parameters for a given specimen by moving horizontally, while comparisons for geometric effects on a given type of parameter can be made by moving vertically from the 30° cone to the cylinder (top to bottom). The latter procedure will be used in the subsequent discussion. Although the absolute values of the parameters are plotted, the algebraic sign is indicated for the various branches of the curves. These algebraic signs, of course, correspond to the convention indicated in Figure 2. Experimental phase angles were found to correspond with these signs in general, except that they shifted more gradually in the vicinity of discontinuities, because of the presence of damping.

The translational velocity ratio (Figs. 7-9) and the rotational velocity ratio (Figs. 10-12) were included as parameters since they are probably the least susceptible to errors within the experimental apparatus. That is, the signals were obtained simply from piezoelectric accelerometers, and no further processing other than filtering was applied. Likewise, these

30° Cone					
7	10	13	16	19	22
$\dot{V}_2/\dot{V}_1$	$\dot{\Psi}_2/\dot{V}_1$	$Q_1/\dot{V}_1$	$M_1/\dot{V}_1$	$Q_1/\dot{V}_2$	$M_1/\dot{V}_2$
15° Cone					
8	11	14	17	20	23
$\dot{V}_2/\dot{V}_1$	$\dot{\Psi}_2/\dot{V}_1$	$Q_1/\dot{V}_1$	$M_1/\dot{V}_1$	$Q_1/\dot{V}_2$	$M_1/\dot{V}_2$
Cylinder					
9	12	15	18	21	24
$\dot{V}_2/\dot{V}_1$	$\dot{\Psi}_2/\dot{V}_1$	$Q_1/\dot{V}_1$	$M_1/\dot{V}_1$	$Q_1/\dot{V}_2$	$M_1/\dot{V}_2$

Figure 6. Convenient Layout For Results

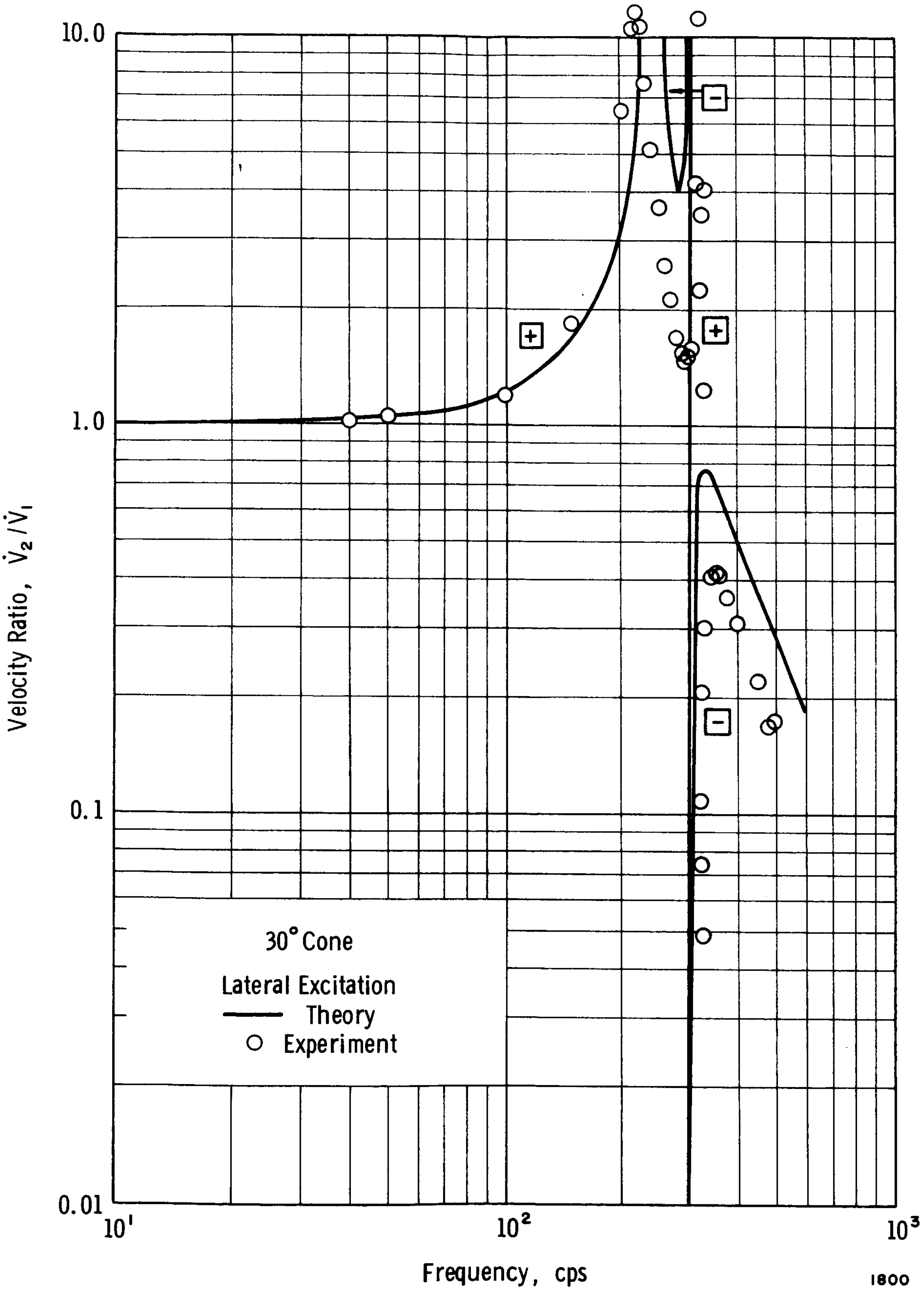

Figure 7. Translational Velocity Ratio For 30° Cone And Top Mass

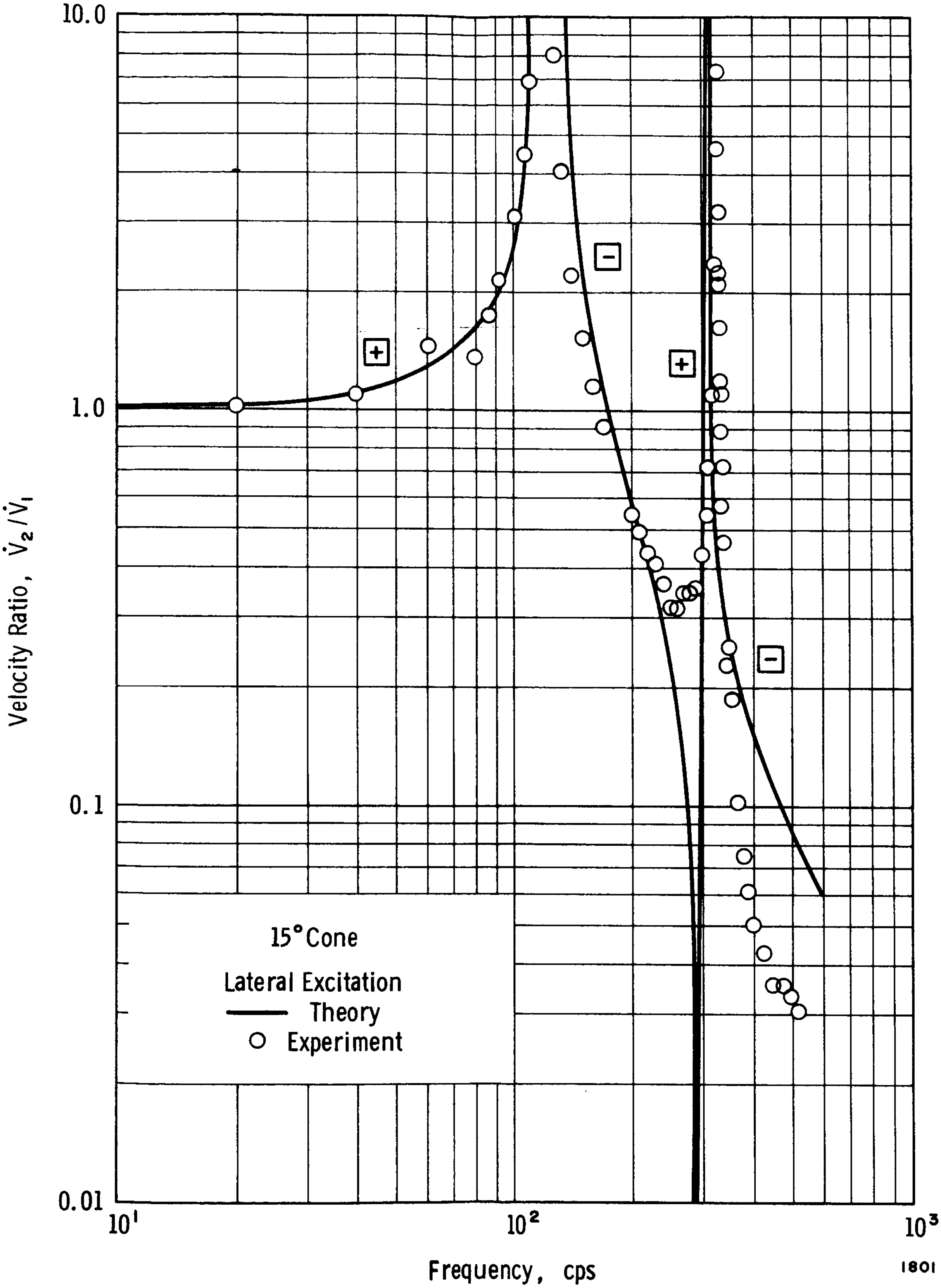

Figure 8. Translational Velocity Ratio For 15° Cone And Top Mass

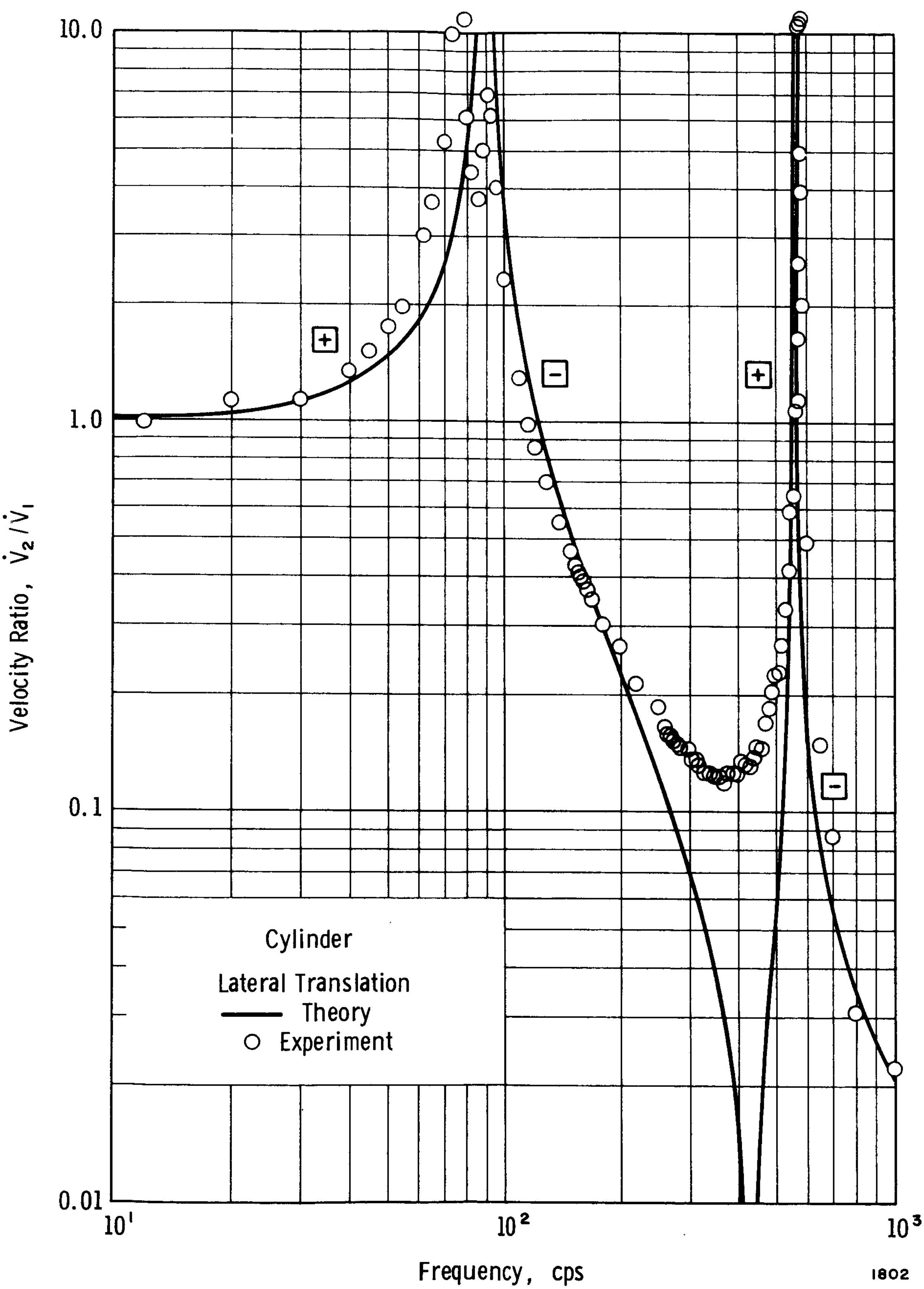

Figure 9. Translational Velocity Ratio For Cylinder And Top Mass

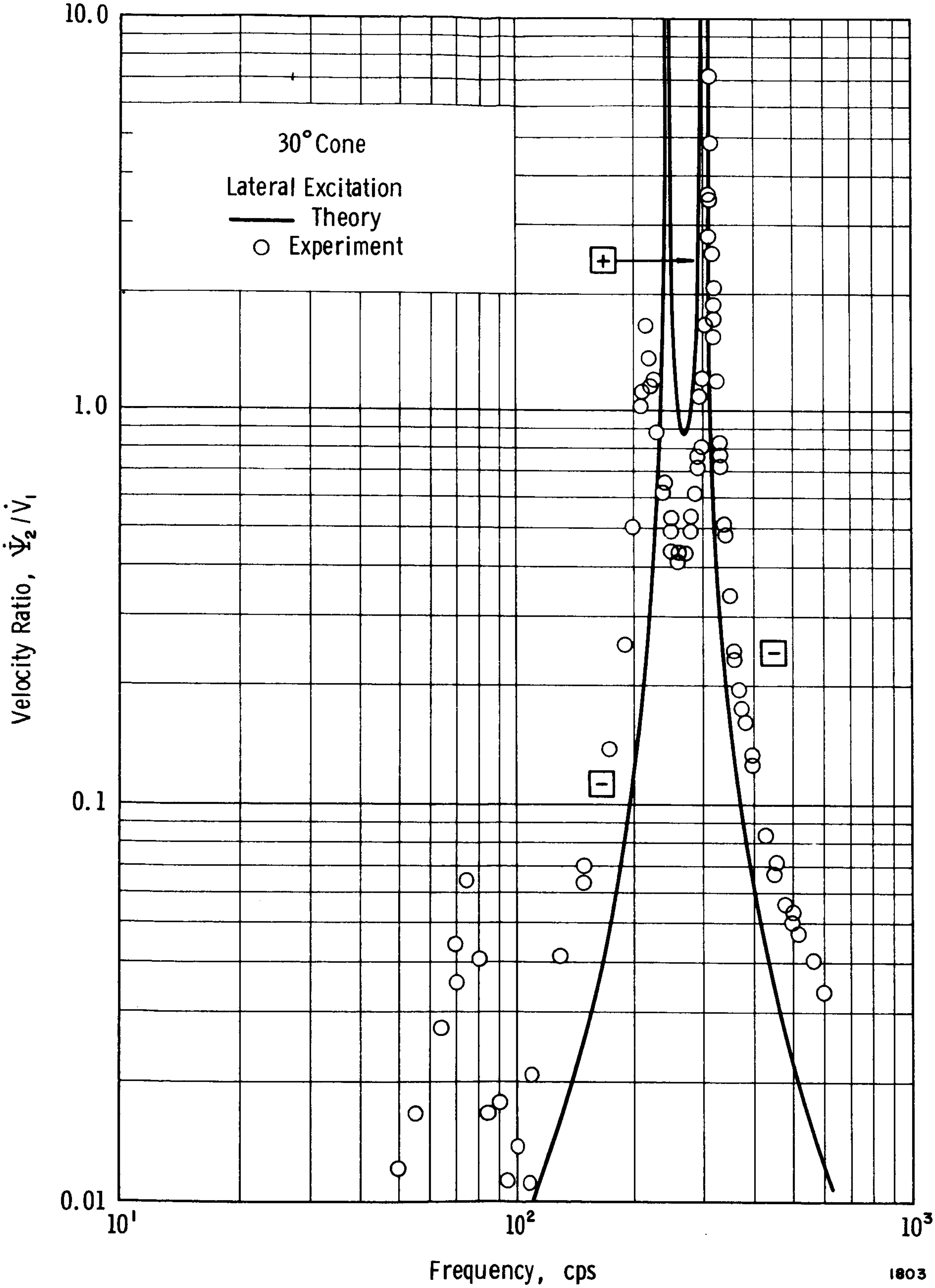

Figure 10. Rotational Velocity Ratio For 30° Cone And Top Mass

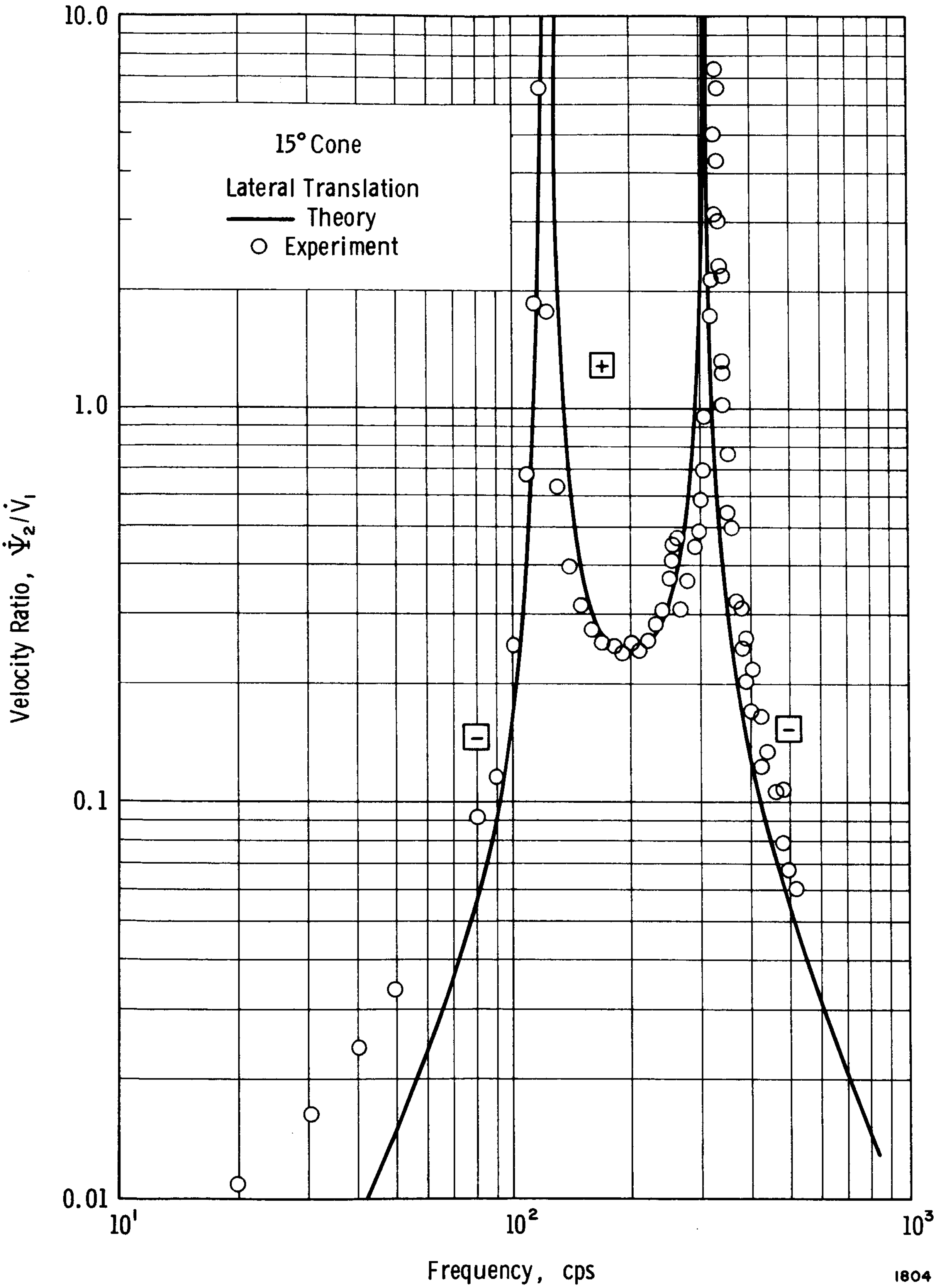

Figure 11. Rotational Velocity Ratio For 15° Cone And Top Mass

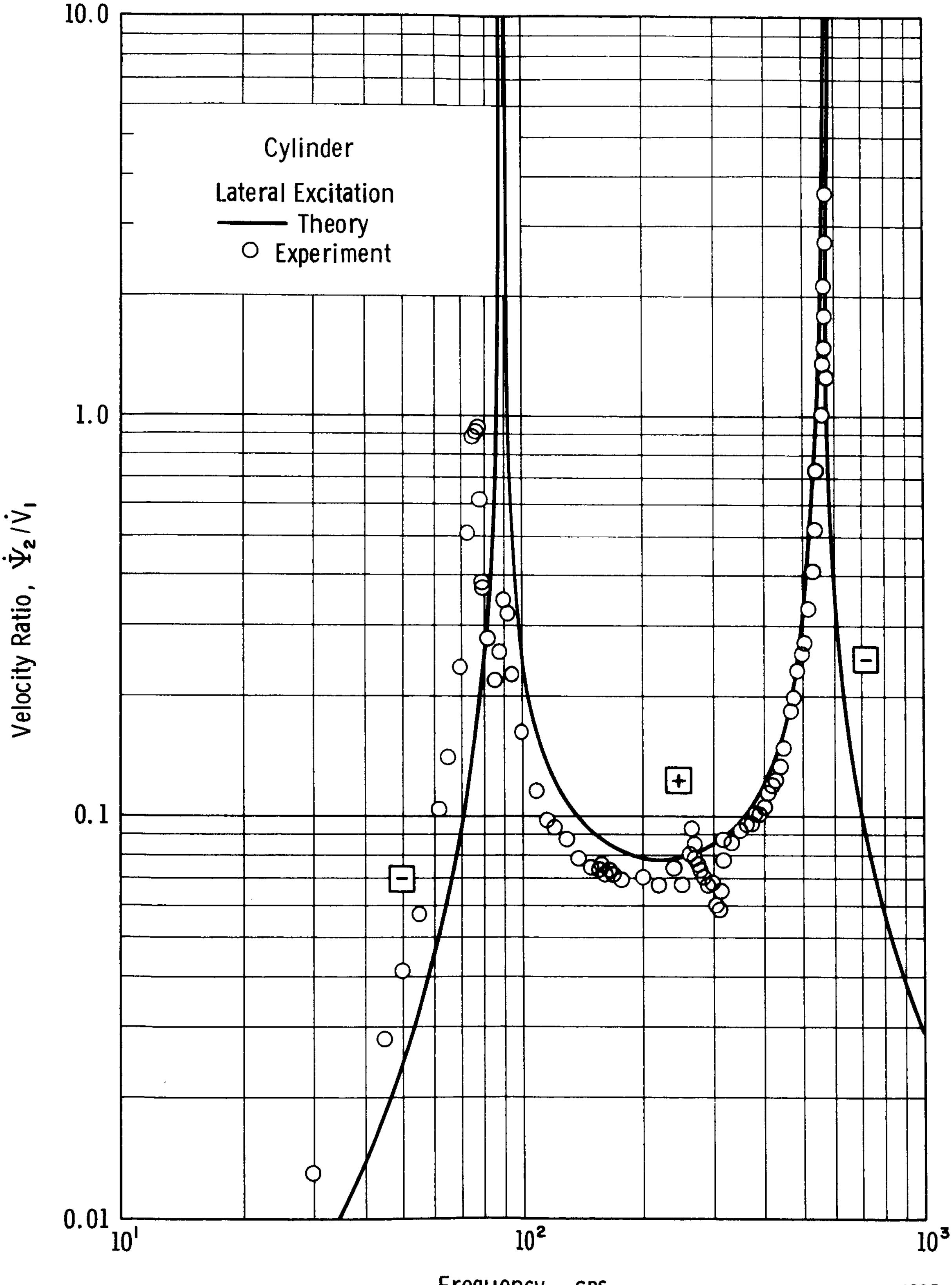

Figure 12. Rotational Velocity Ratio For Cylinder And Top Mass

signals, as well as those for moments, were not influenced by the mass-balance system. Division in the velocity ratios, as for all cases, was performed numerically rather than electronically. A basic change in the trend of the translational velocity ratio occurs in going from the 30° cone (Fig. 7) to the 15° cone (Fig. 8). The 15° cone and cylinder are more alike (Figs. 8, 9).

Overall agreement between theory and experiment is good for the first two parameters (Figs. 7-9 and 10-12), although various discrepancies can be observed in different areas of the frequency range. The first resonance appears to occur at a slightly lower frequency than predicted for all three geometries. In addition, a split peak, which probably results from geometric defects, occurs for the first resonance in the cylinder. This trend will be consistent throughout all the results. It may be noted that an extraneous resonance appeared at about 75 cps in Figure 10. This resonance does not appear in any of the other data for the 30° cone and is probably due to extraneous motion in some part of the fixtures that did not influence the other signals.

Force input pseudoimpedances are shown in Figures 13-15. Again a basic change in the trend occurs in going from the 30° cone (Fig. 13) to the 15° cone (Fig. 14). Comparison between theory and experiment is good outside the two resonance peaks, but is poor for the range of frequencies in between. The discrepancy appears to be most severe for the cylinder, where the experimental intermediate antiresonance occurs at a significantly lower frequency than is predicted. The source of this

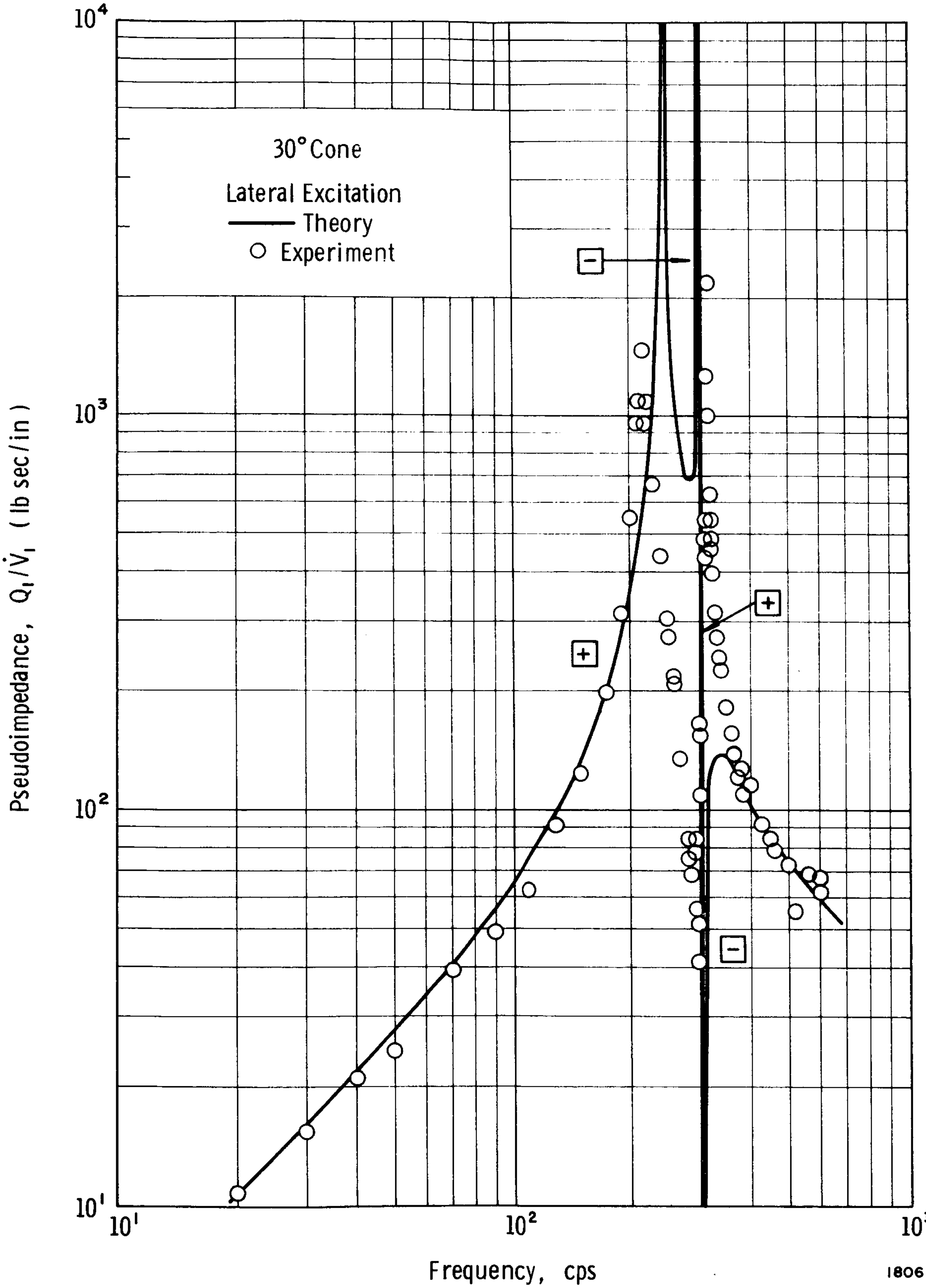

Figure 13. Force Input Pseudoimpedance For 30° Cone And Top Mass

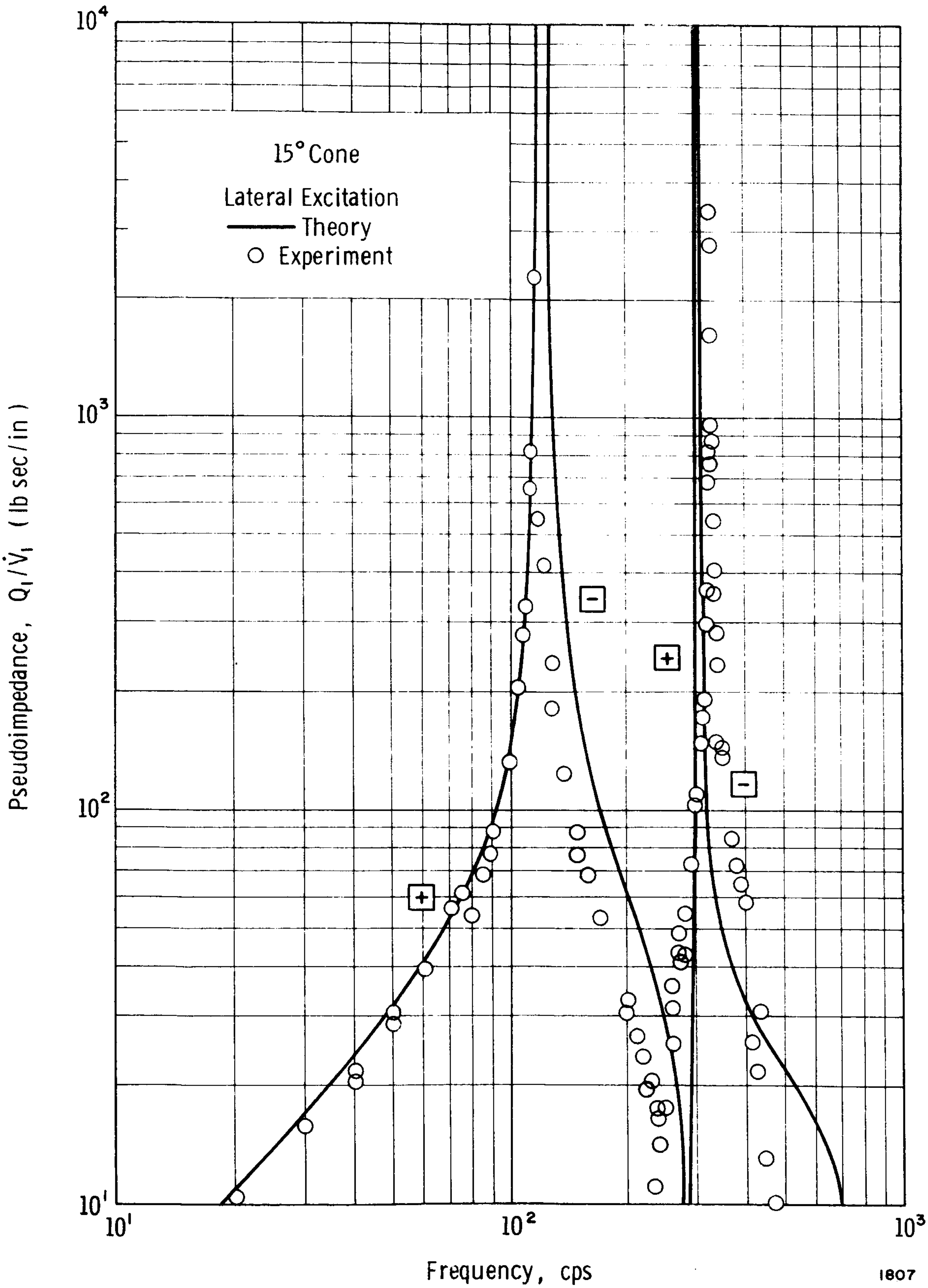

Figure 14. Force Input Pseudoimpedance For 15° Cone And Top Mass

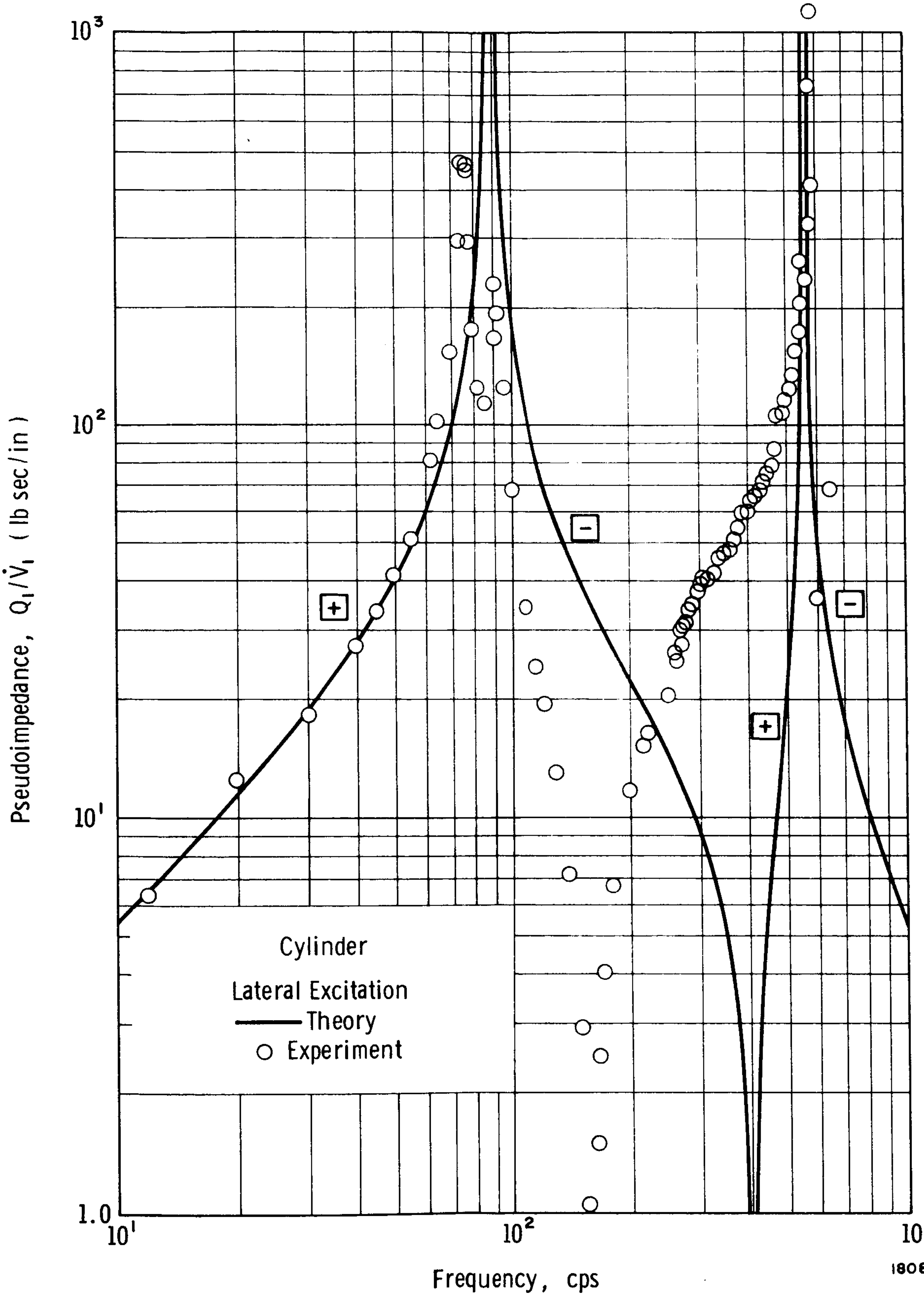

Figure 15. Force Input Pseudoimpedance For Cylinder And Top Mass

error appears to be in the value of the net shear force Q_1. In order to verify the performance of the experimental system, data were retaken after the system had been disassembled and reassembled, and no essential difference in results occurred. Further, the performance of the mass-balance system was checked and rechecked. The linearity of the system was found to be good upon checking the results at various input amplitudes. Thus, the source of the discrepancy does not appear to lie in the instrumentation.

Further reflection on the location of the antiresonance in Figures 13-15 leads back to Eq. (10b). That is, the antiresonance occurs at the point where the net shear force Q_1 at the input becomes zero. Theoretically, this occurs in the nontrivial case where the two terms of Eq. (10b) nullify each other. It appears that in the experimental system, the actual distribution of shear forces present is different from that predicted within the intermediate frequency range. This may result from small wrinkles and eccentricities in the cylinder or may reflect the need of using a bending theory. More work is necessary to resolve this question.

Moment input pseudoimpedance is shown in Figures 16-18. Although there is a consistent change in shape in going from the 30° cone to the cylinder, the general character of the curves is unaltered. Agreement between theory and experiment appears to be worst for the 15° cone, with a local extraneous discontinuity appearing at about 250 cps. The origin of this discontinuity remains undetermined. We again emphasize that this parameter was not influenced by the mass-balance system.

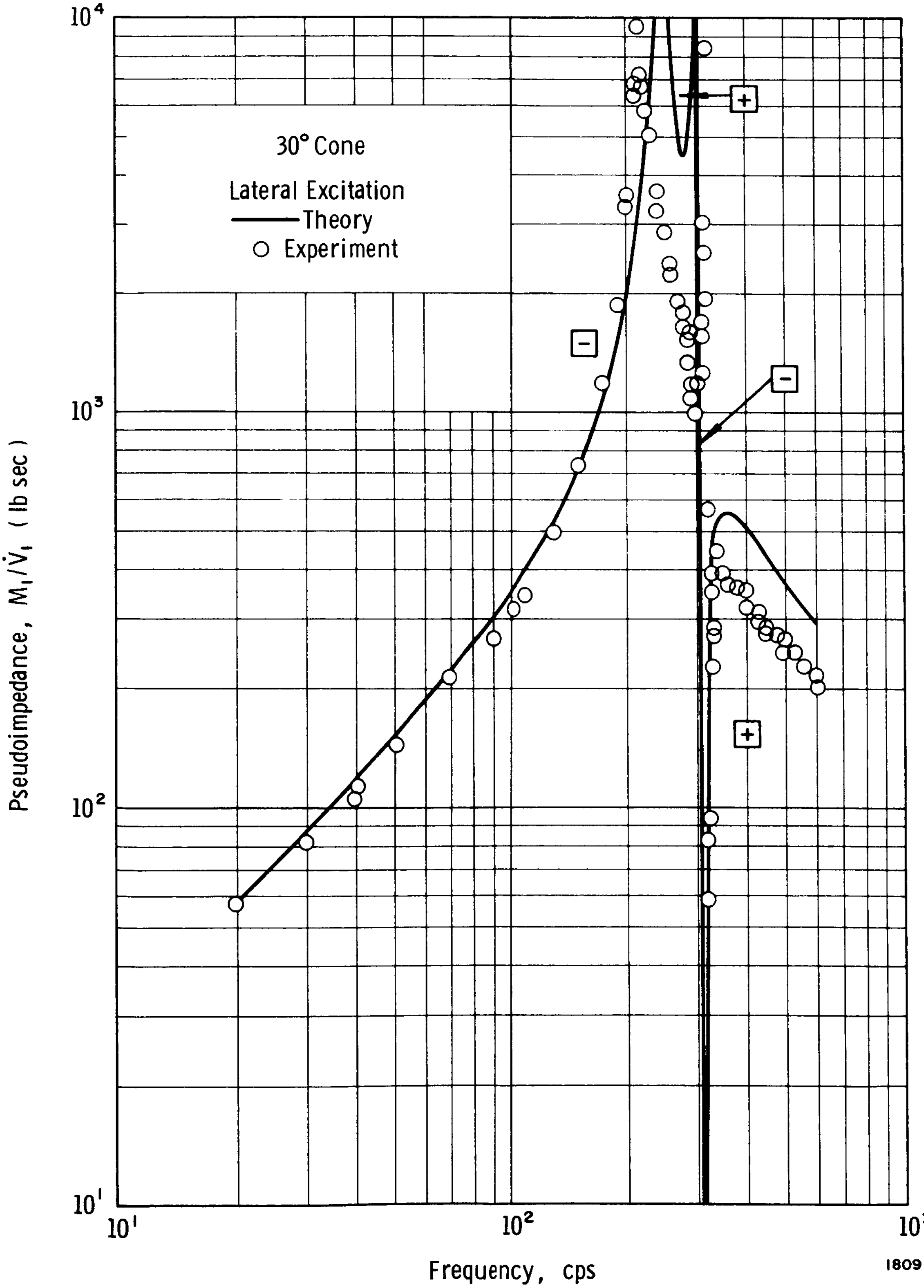

Figure 16. Moment Input Pseudoimpedance For 30° Cone And Top Mass

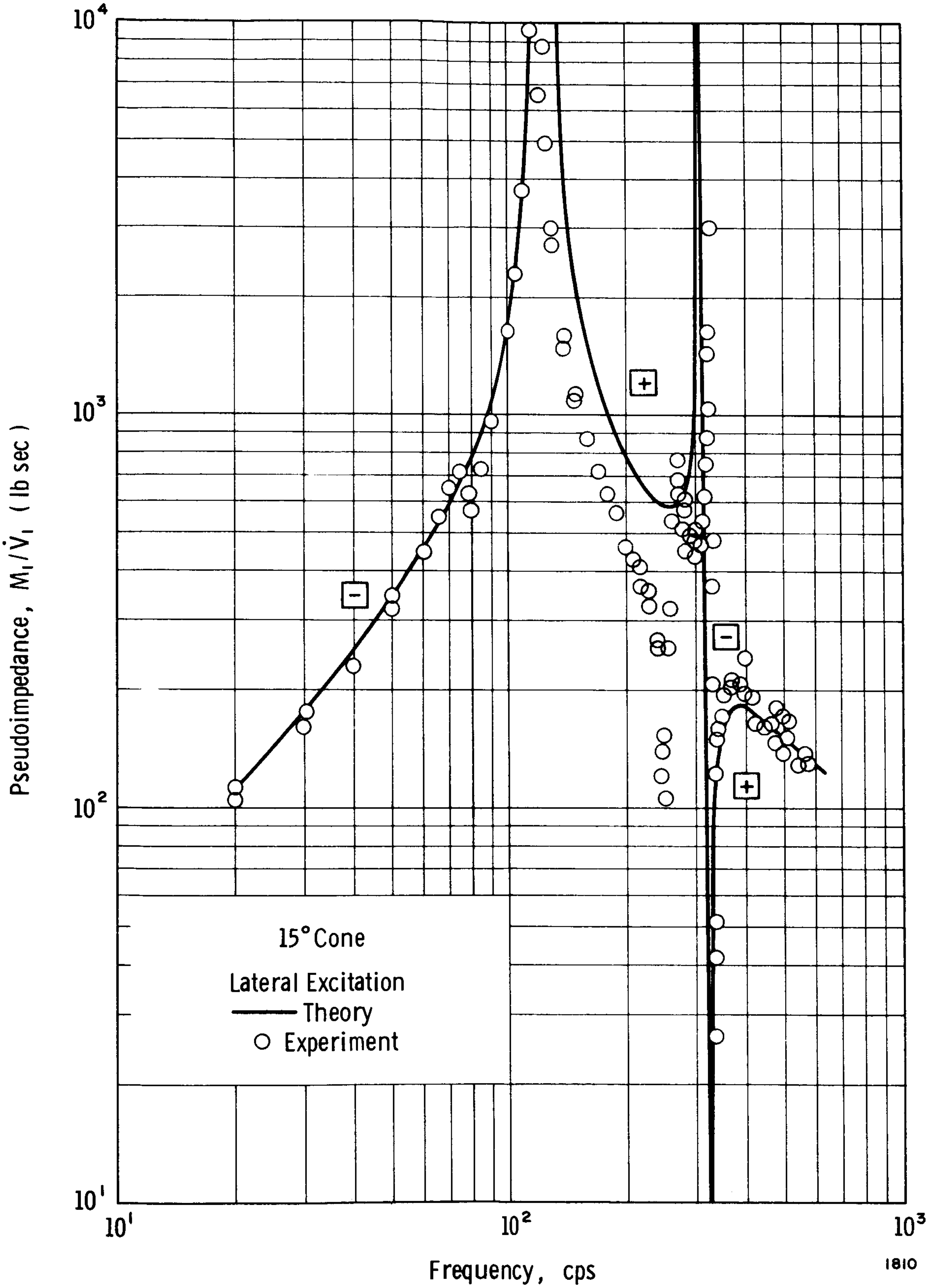

Figure 17. Moment Input Pseudoimpedance For 15° Cone And Top Mass

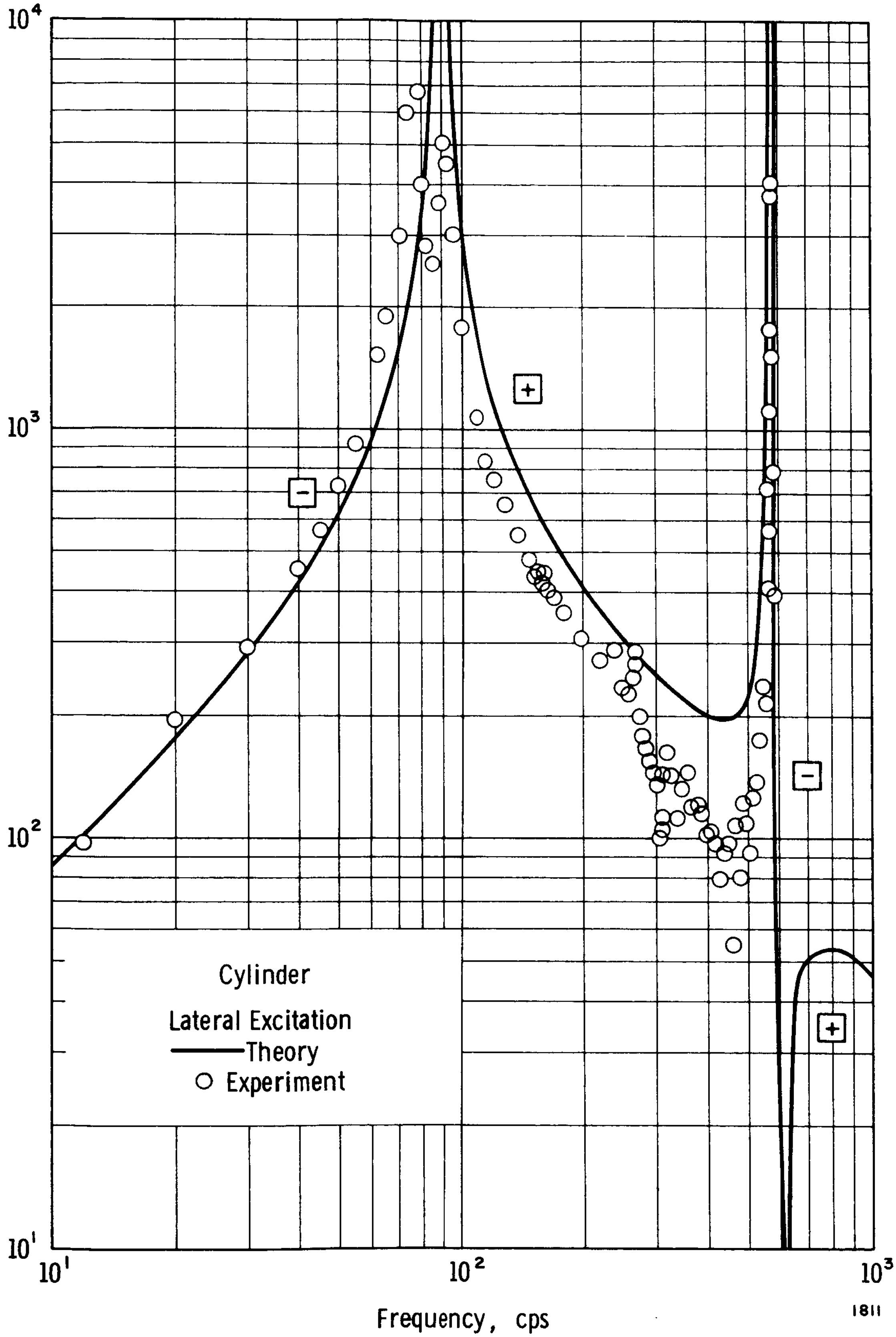

Figure 18. Moment Input Pseudoimpedance For Cylinder And Top Mass

Force transfer pseudoimpedance is shown in Figures 19-21. Agreement between theory and experiment is quite good for the 30° cone, but becomes progressively worse in going to the cylinder. Again the increasing discrepancy in the position of the intermediate antiresonance appears. Figure 21 probably shows the worst overall correspondence for all the data presented. The same comments which were previously made about this discrepancy also apply here.

Moment transfer pseudoimpedance is shown in the final Figures 22-24. Agreement between theory and experiment is fair. Again the extraneous discontinuity appears in the experimental values for the 15° cone at about 250 cps. Likewise, increased discrepancy occurs above 400 cps.

Several possible sources of error in the experiments have already been mentioned but were continuously checked. An additional source, however, is inability to maintain a perfect zero rotational input ($\Psi_1 = 0$) at the base of the specimens. The sensitivity of the results to small amplitudes of this parameter would need to be determined.

Overall agreement in all results appears to be good. However, several definite discrepancies are present for part of the frequency range. Whether or not the use of a bending theory would prove more accurate, or whether consideration must be given to cylinder imperfections, remains to be determined. Nevertheless, the membrane theory does appear to provide at least a good approximation for predicting impedance and transmission characteristics of cones and cylinders.

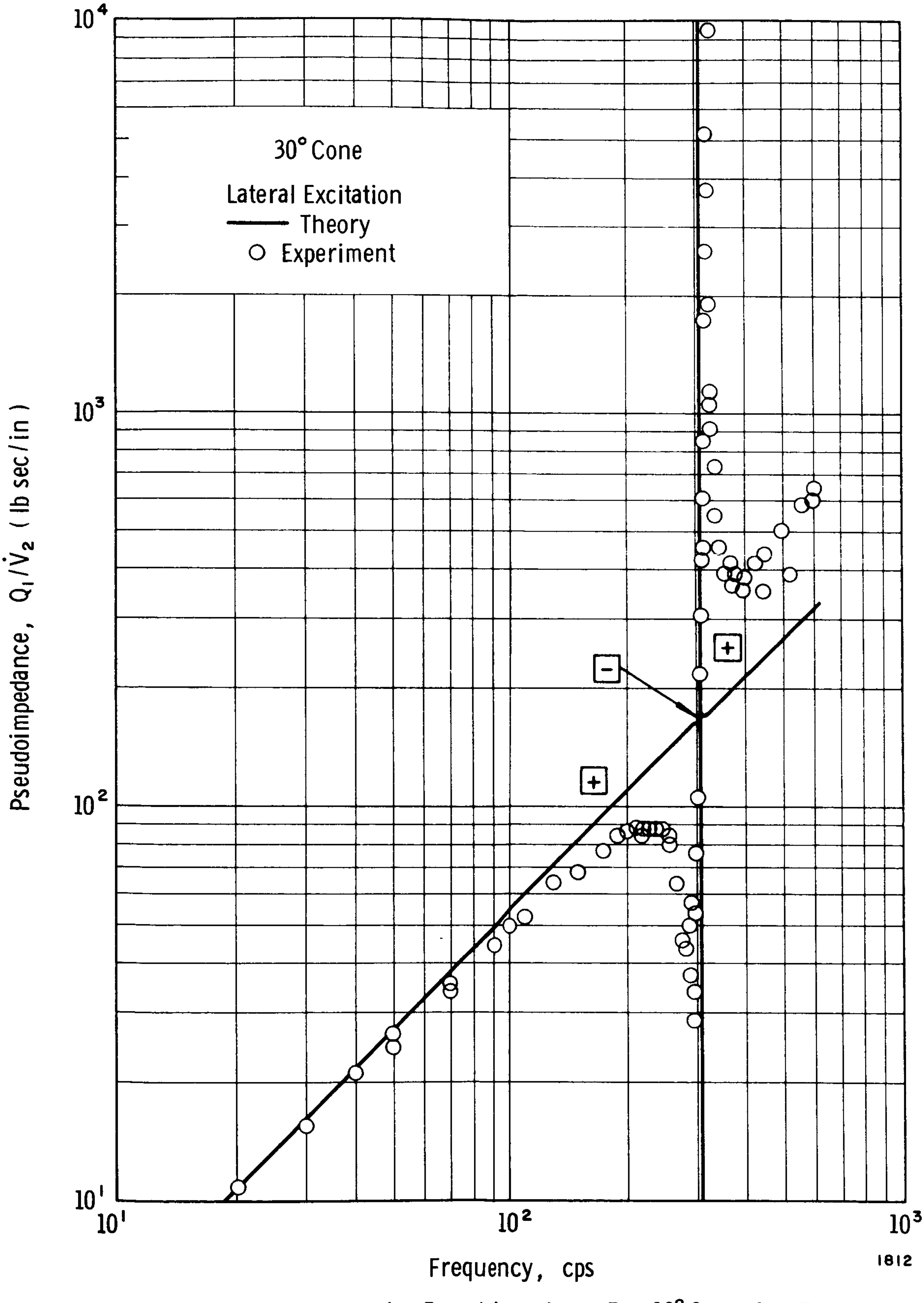

Figure 19. Force Transfer Pseudoimpedance For 30° Cone And Top Mass

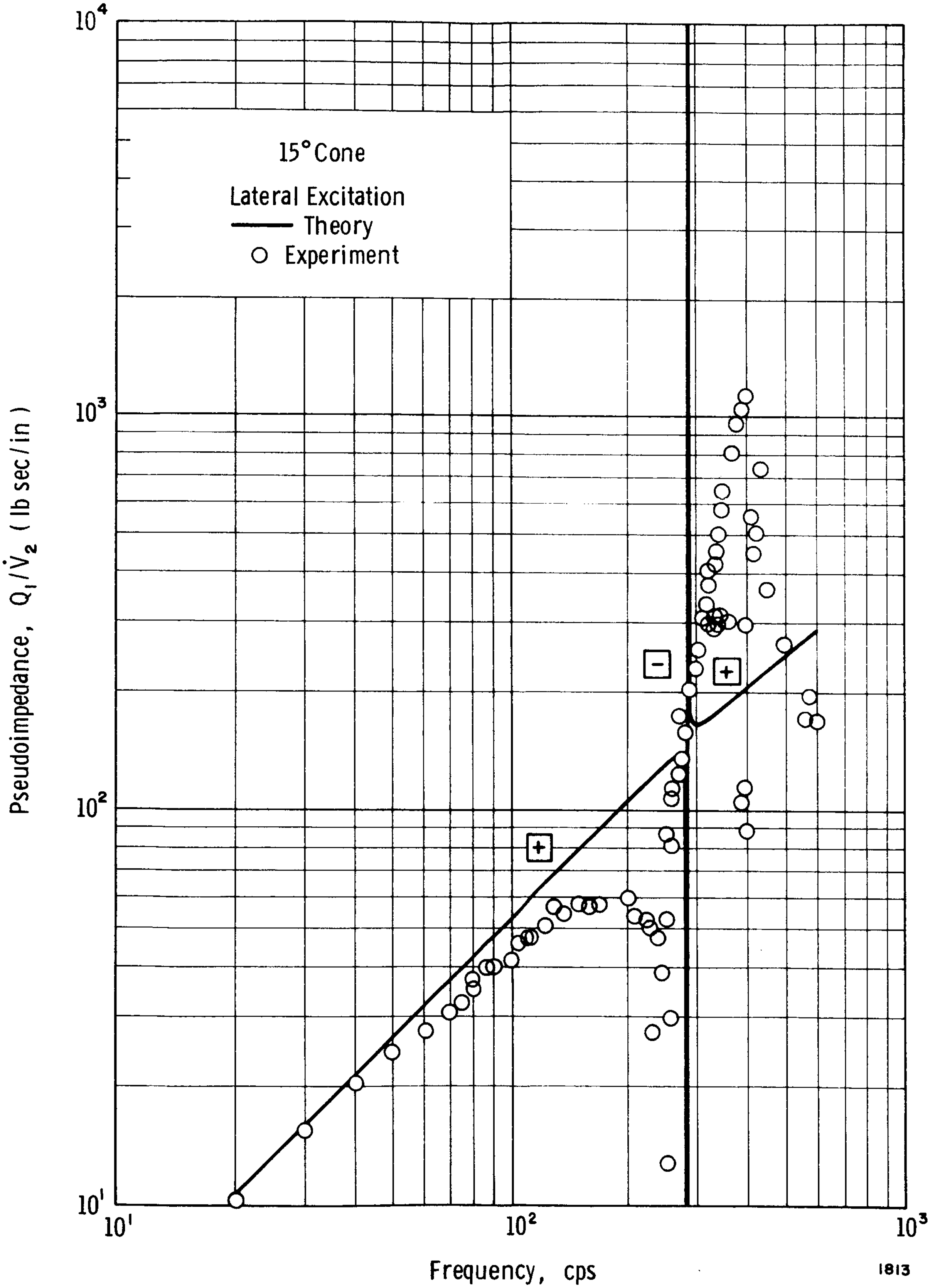

Figure 20. Force Transfer Pseudoimpedance For 15° Cone And Top Mass

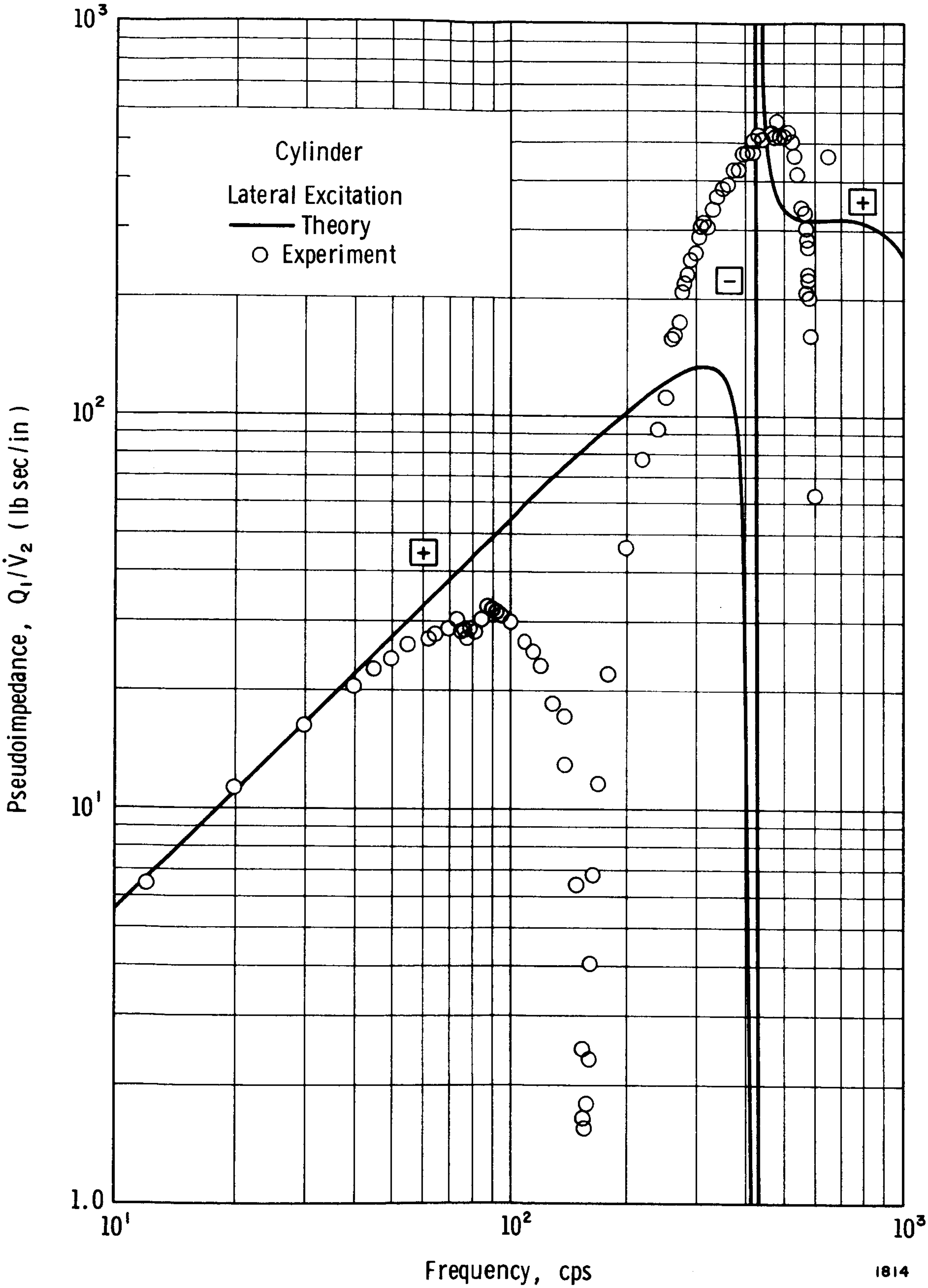

Figure 21. Force Transfer Pseudoimpedance For Cylinder And Top Mass

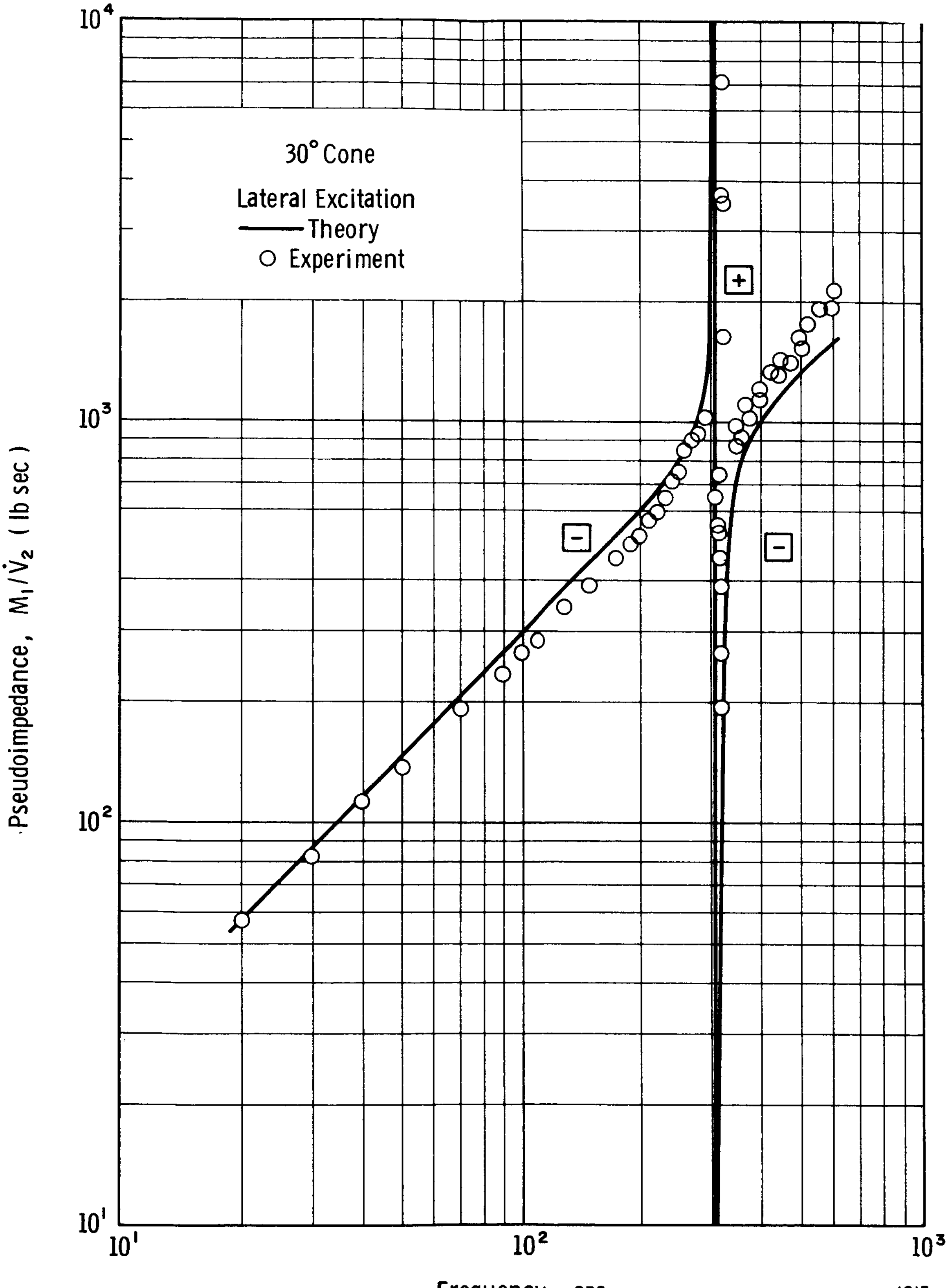

Figure 22. Moment Transfer Pseudoimpedance For 30° Cone And Top Mass

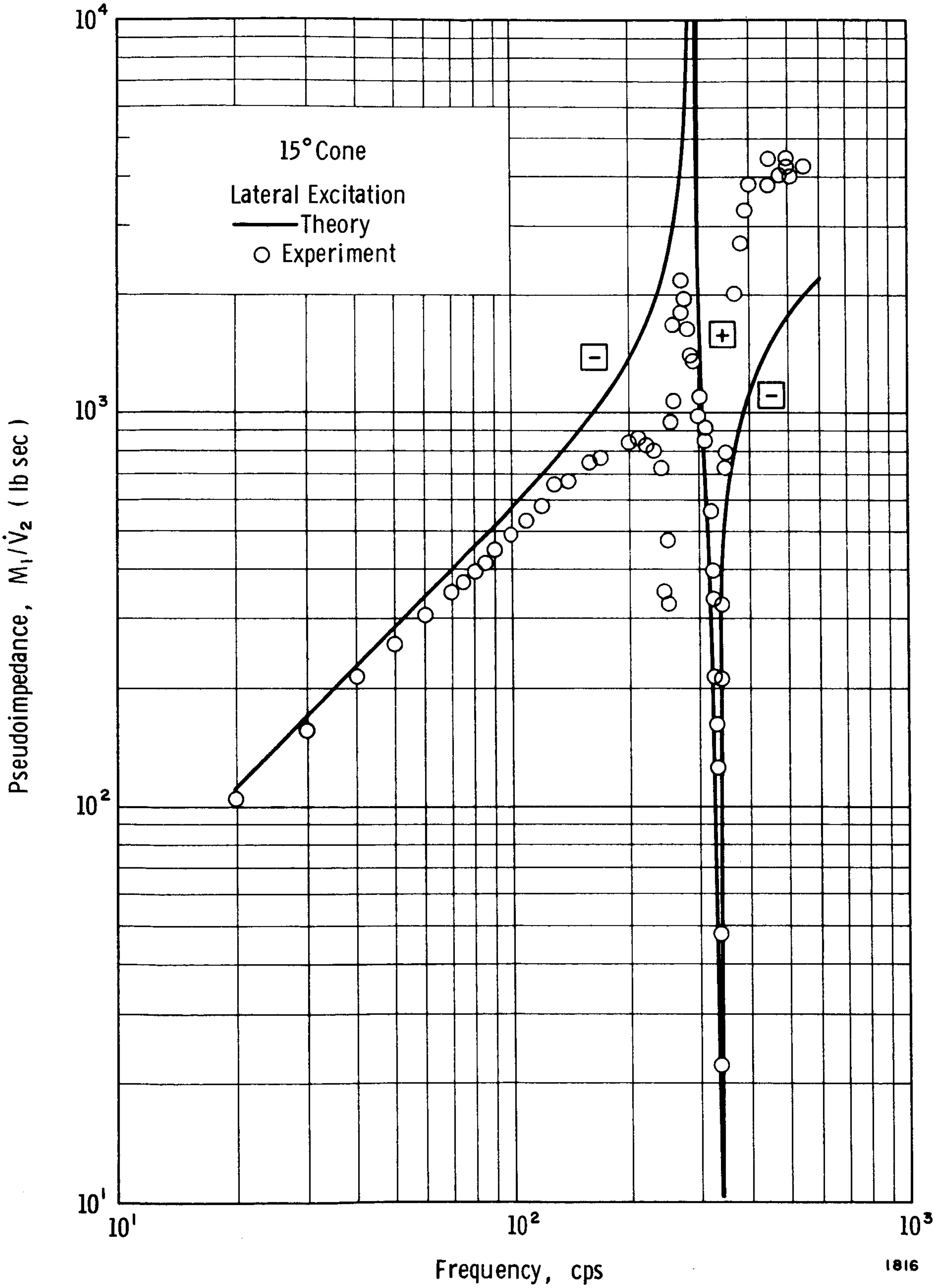

Figure 23. Moment Transfer Pseudoimpedance For 15° Cone And Top Mass

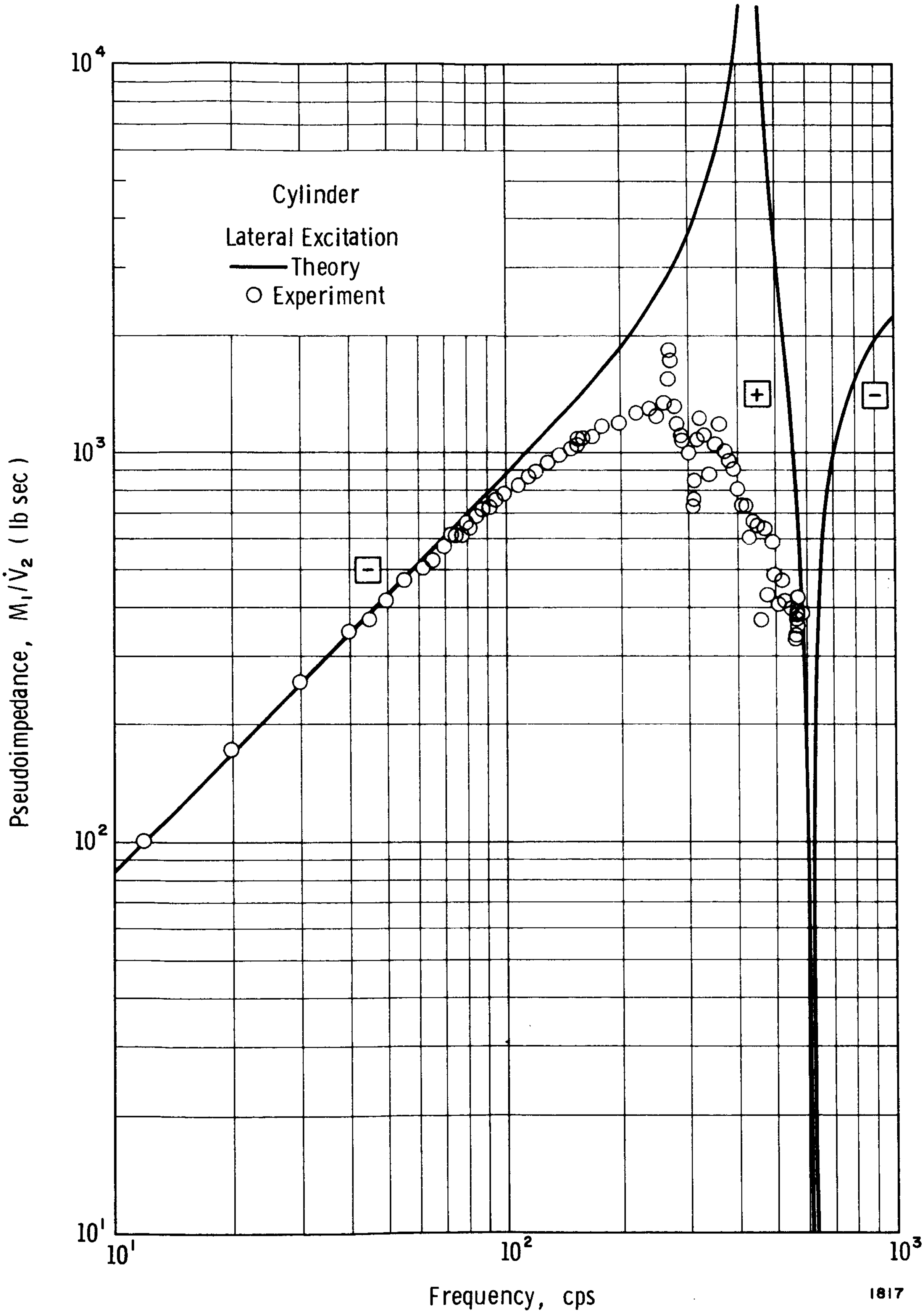

Figure 24. Moment Transfer Pseudoimpedance For Cylinder And Top Mass

ACKNOWLEDGMENTS

This work was sponsored by NASA Goddard Space Flight Center through Contract NAS 5-10312. The authors sincerely thank Mr. J.P. Young for constructive discussions and comments, and Drs. H. N. Abramson and U. S. Lindholm for consultation and general support during this research. They also gratefully thank Messrs. R. E. Gonzales and D. C. Scheidt for their able assistance with the computer programming and experiments, respectively.

REFERENCES

1. Hu, W. C. L. and Kana, D. D., "Impedance Characteristics of Conical Shells Under Axial Excitations," Final Report, Part I, Contract NAS 5-10312, Southwest Research Institute, San Antonio, Texas, May 1967.

2. Kana, D. D. and Hu, W. C. L., "Impedance Characteristics of Conical Shells Under Lateral Excitations," Third Quarterly Report, Contract NAS 5-10312, Southwest Research Institute, San Antonio, Texas, September 1967.

3. Rubin, S., "Transmission Matrices for Vibration and Their Relation to Admittance and Impedance," Journal of Engineering for Industry, pp. 9-21, February 1964.

4. Rubin, S., "Mechanical Immittance- and Transmission-Matrix Concepts," Jour. of the Acous. Soc. of Amer., Vol. 41, No. 5, pp. 1171-1179, 1967.

5. O'Hara, G. J., "Mechanical Impedance and Mobility Concepts," Jour. of the Acous. Soc. of Amer., Vol. 41, No. 5, pp. 1180-1184, 1967.

6. On, F. J., "Mechanical Impedance Analysis for Lumped Parameter Multi-Degree of Freedom/Multi-Dimensional Systems," NASA TN D-3865, May 1967.

7. Simmonds, J. G., "Modifications of the Timoshenko Beam Equations Necessary for Thin-Walled Circular Tubes," Int. J. Mech. Sci. Pergamon Press Ltd., Vol. 9, No. 5, 11. 237-244, May 1967.

APPENDIX

LISTING OF COMPUTER PROGRAM AND FORMAT OF INPUT DATA CARDS

INPUT DATA DESCRIPTION
(CONE)

CARD NO.	FORTRAN SYMBOL	VARIABLE NAME	UNITS	DEFINITION
1	N	n		Number of frequency sets.
2	A	a	in.	Major base radius.
	SB	b	in.	Minor base radius.
	ALPHA		deg.	Semivertex angle.
	H	h	in.	Wall thickness of conical shell.
3	ENU	ν		Poisson's ratio.
	E	E	psi	Young's modulus.
	RHO	ρ	lb-sec^2/in^4	Mass density.
4	WT	W_t	lb.	Weight of attached mass.
	AI	I	lb-in-sec^2	Moment of inertia of supported mass.
	DEL	δ	in.	Offset of center of supported mass.
5	FRQ_i	f_i	cps	Initial frequency.
	$FRQX_i$	Δf_i	cps	Frequency increment.
	$FRQN_i$	f_n	cps	Final frequency.

PROGRAM OUTPUT

Printed Output

1. All input data except I and δ.
2. Frequency f in cps and rad/sec.
3. Characteristic transfer matrix $[\alpha_{ij}]$ and transfer matrix $[\beta_{ij}]$.
4. Translational and rotational velocity ratios $(\dot{V}_2/\dot{V}_1)$ and $(\dot{\Psi}_2/\dot{V}_1)$.
5. Force input and moment input pseudo impedances ZQ11 and ZM11.
6. Force transfer and moment transfer pseudo impedances ZQ12 and ZM12.
7. If $\Omega > \cos(\alpha)$, an error message will be printed and the program will continue.

PROGRAM NOTES
(CONE)

Subprogram Used

In addition to the main program, the following function subprogram was used.

1. RKLDEQ, computes the solution of n first-order ordinary differential equations by the Runge-Kutta-Gill fourth-order method.

```
C     PROGRAM CYLINDER
C     SWRI PROJECT 02-2034
C     CDC 3600 FORTRAN
      DIMENSION F(12),FDX(12),FN(12)
      DIMENSION A(4,4),B(4,4),C(4,4),IROW(5),ICOL(5)
      DATA (PI=3.1415926 5),(C1=386.0)
 2000 READ 200, N
  200 FORMAT ( I5 )
      IF (EOF,60)20,25
   20 STOP
C *** GEOMETRIC PARAMETERS
   25 READ 205, SA,SL,H
  205 FORMAT ( 3F10.0 )
C *** MATERIAL PARAMETERS
      READ 210, ENU,E,RHO
  210 FORMAT (F10.0,2E10.2)
C *** RIGID MASS
      READ 215, WT,AI,DEL
  215 FORMAT ( 3F10.0 )
      BMS = WT/C1
      ALPHA = 0.
      SB = SA
C *** FREQUENCY RANGE
      READ 205, (F(I),FDX(I),FN(I),I=1,N)
      PRINT 300
  300 FORMAT (1H1, 6X,55HCYLINDRICAL SHELL LATERAL IMPEDANCE PROGRAM - D
     1.D. KANA//66H THIS PROGRAM CALCULATES (4X4) TRANSMISSION MATRICES
     2BETA(I,J) AND/66H ALPHA(I,J) FOR CYLINDRICAL SHELLS UNDER LATERAL
     3EXCITATIONS, ALSO/66H CALCULATES INPUT AND TRANSFER PSEUDO IMPEDAN
     4CES WHEN AN ARBITRARY/44H MASS M IS ATTACHED TO THE OUTPUT TERMINA
     5L 2)
      PRINT 305,ALPHA,E,SA,ENU,SB,RHO,H,BMS
  305 FORMAT (1H0,10X,20HGEOMETRIC PARAMETERS,25X,19HMATERIAL PARAMETERS
     1/26H SEMIVERTEX ANGLE ALPHA = ,F7.3, 8H DEGREES,6X,20HYOUNGS MODUL
     2US   E = ,E10.3, 4H PSI/26H MAJOR BASE RADIUS     A = ,F7.3,7H INCHE
     3S,7X,20HPOISSONS RATIO NU = ,E10.3/26H MINOR BASE RADIUS     B = ,
     4F7.3, 7H INCHES,7X,20HMASS DENSITY   RHO = ,E10.3,17H LB(SEC)**2/IN
     5**4/10H THICKNESS,12X, 4HH = ,F7.3, 7H INCHES,7X, 4HMASS,12X, 4HM
     6= ,E10.3,14H LB(SEC)**2/IN)
      PRINT 320
  320 FORMAT (1H0,34X,17HFREQUENCY ( CPS ))
      PRINT 325, (F   (I),FDX (I),FN   (I),I=1,N)
  325 FORMAT (30X,F8.1,2H (,F6.1,2H ),F8.1)
      PRINT 330
  330 FORMAT (*0  FREQ*,5X,*OMEGA*,14X,*((ALPHA(I,J),J=1,4),I=1,4)*,
     1  27X,*((BETA(I,J),J=1,4),I=1,4)*)
      G = E/(2.0*(1.0+ENU))
      W0 = SQRTF(E/RHO)/SA
      DO 40 I=1,N
      FREQ = F(I)
 1000 W = 2.0*PI*FREQ
      WSQ = W*W
      OMEGA = W/W0
      OSQ = OMEGA*OMEGA
      ARG = SQRTF(0.5/(1.0+ENU))
      IF (OMEGA.LT.ARG)11,12
   11 SGN = 1.0
      GO TO 10
   12 IF (OMEGA.GT.ARG.AND.OMEGA.LT.0.99)13,15
   13 SGN = -1.0
   10 P = (OSQ/(2.0*(1.0-OSQ)))*(5.0+2.0*ENU-(1.0+ENU)*(3.0-ENU)*OSQ)
      Q = (OSQ/(1.0-OSQ))*(1.0-2.0*(1.0+ENU)*OSQ)*(2.0-(1.0-ENU*ENU)*
```

```
     1  OSQ)                                                           SWR 6400
      DIS = SQRTF(P*P+Q)                                               SWR 6500
      AL1 = SQRTF(P+DIS)                                               SWR 6600
      AL2 = SQRTF((-P+DIS)*SGN)                                        SWR 6700
      VI1 = (AL1*SL)/SA                                                SWR 6800
      VI2 = (AL2*SL)/SA                                                SWR 6900
      F1 = (ENU*AL1*AL1-1.0-2.0*ENU*(1.0+ENU)*OSQ)/(1.0-(1.0+ENU)**2*  SWR 7000
     1  OSQ)                                                           SWR 7100
      F2 = (-ENU*SGN*AL2*AL2-1.0-2.0*ENU*(1.0+ENU)*OSQ)/(1.0-(1.0+     SWR 7200
     1  ENU)**2*OSQ)                                                   SWR 7300
      G1 = ((1.0-ENU*ENU)*OSQ*F1-F1-1.0)/(ENU*AL1)                     SWR 7400
      G2 = ((1.0-ENU*ENU)*OSQ*F2-F2-1.0)/(ENU*AL2)                     SWR 7500
      U1 = (G1*AL1+ENU+ENU*F1)*((PI*SA*E*H )/(1.-ENU**2))              SWR 7600
      U2 = (G2*AL2+ENU+ENU*F2)*((PI*SA*E*H)/(1.-ENU**2))               SWR 7700
      U3 = PI*G*H*(AL1+G1)                                             SWR 7800
      U4 = PI*G*H*(AL2-G2)                                             SWR 7900
      U5 = PI*G*H*(AL2+G2)                                             SWR 8000
      A(1,1) = 0.                                                      SWR 8100
      A(1,2) = U3                                                      SWR 8200
      A(1,3) = 0.                                                      SWR 8300
      A(1,4) = U4                                                      SWR 8400
      A(2,1) = U1                                                      SWR 8500
      A(2,2) = 0.                                                      SWR 8600
      A(2,3) = U2                                                      SWR 8700
      A(2,4) = 0.                                                      SWR 8800
      A(3,1) = 1.                                                      SWR 8900
      A(3,2) = 0.                                                      SWR 9000
      A(3,3) = 1.                                                      SWR 9100
      A(3,4) = 0.                                                      SWR 9200
      A(4,1) = 0.                                                      SWR 9300
      A(4,2) = -G1/SA                                                  SWR 9400
      A(4,3) = 0.                                                      SWR 9500
      A(4,4) = +G2/SA                                                  SWR 9600
      CN1 = COSF(VI1) $ SN1 = SINF(VI1)                                SWR 9700
      CN2 = COSF(VI2) $SN2 = SINF(VI2)                                 SWR 9800
      SNH = 0.5*(EXPF(VI2)-EXPF(-VI2))                                 SWR 9900
      CSH = 0.5*(EXPF(VI2)+EXPF(-VI2))                                 SWR10000
      B(1,1) = -U3*SN1                                                 SWR10100
      B(1,2) = U3*CN1                                                  SWR10200
      B(2,1) = U1*CN1                                                  SWR10300
      B(2,2) = U1*SN1                                                  SWR10400
      B(3,1) = CN1                                                     SWR10500
      B(3,2) = SN1                                                     SWR10600
      B(4,1) = (G1*SN1)/SA                                             SWR10700
      B(4,2) = -(G1*CN1)/SA                                            SWR10800
      IF (OMEGA.LT.ARG)14,16                                           SWR10900
   14 B(1,3) = U4*SNH                                                  SWR11000
      B(1,4) = U4*CSH                                                  SWR11100
      B(2,3) = U2*CSH                                                  SWR11200
      B(2,4) = U2*SNH                                                  SWR11300
      B(3,3) = CSH                                                     SWR11400
      B(3,4) = SNH                                                     SWR11500
      B(4,3) = (G2*SNH)/SA                                             SWR11600
      B(4,4) = (G2*CSH)/SA                                             SWR11700
      GO TO 17                                                         SWR11800
   16 IF (OMEGA.GT.ARG.AND.OMEGA.LT.0.99)18,15                         SWR11900
   18 B(1,3) = -U5*SN2                                                 SWR12000
      B(1,4) = +U5*CN2                                                 SWR12100
      B(2,3) = U2*CN2                                                  SWR12200
      B(2,4) = U2*SN2                                                  SWR12300
      B(3,3) = CN2                                                     SWR12400
      B(3,4) = SN2                                                     SWR12500
```

```
      B(4,3) = (G2*SN2)/SA                                              SWR12600
      B(4,4) = -(G2*CN2)/SA                                             SWR12700
      A(1,4) = U5                                                       SWR12800
      A(4,4) = -G2/SA                                                   SWR12900
   17 CALL MATINV(A,IROW,ICOL,4,4,1.0E-05)                              SWR13000
      DO 60 J=1,4                                                       SWR13100
      DO 65 K=1,4                                                       SWR13200
      SUM = 0.                                                          SWR13300
      DO 70 L=1,4                                                       SWR13400
      SUM = SUM+B(J,L)*A(L,K)                                           SWR13500
   70 CONTINUE                                                          SWR13600
      C(J,K) = SUM                                                      SWR13700
   65 CONTINUE                                                          SWR13800
   60 CONTINUE                                                          SWR13900
      B11 = C(1,1)                                                      SWR14000
      B12 = C(1,2)                                                      SWR14100
      B13 = C(1,3)                                                      SWR14200
      B14 = C(1,4)                                                      SWR14300
      B21 = C(2,1)                                                      SWR14400
      B22 = C(2,2)                                                      SWR14500
      B23 = C(2,3)                                                      SWR14600
      B24 = C(2,4)                                                      SWR14700
      B31 = C(3,1)                                                      SWR14800
      B32 = C(3,2)                                                      SWR14900
      B33 = C(3,3)                                                      SWR15000
      B34 = C(3,4)                                                      SWR15100
      B41 = C(4,1)                                                      SWR15200
      B42 = C(4,2)                                                      SWR15300
      B43 = C(4,3)                                                      SWR15400
      B44 = C(4,4)                                                      SWR15500
      A11 = B11 $ A12 = B12 $ A21 = B21 $ A22 = B22                     SWR15600
      A31 = W*B31 $ A41 = W*B41 $ A32 = W*B32 $ A42 = W*B42             SWR15700
      A13 = -B13/W $ A23 = -B23/W $ A14 = -B14/W $ A24 = -B24/W         SWR15800
      A33 = B33 $ A34 = B34 $ A43 = B43 $ A44 = B44                     SWR15900
      TM1 = RMS*WSQ                                                     SWR16000
      TM2 = AI*WSQ                                                      SWR16100
      TM3 = TM1*DEL                                                     SWR16200
      C11 = B13+TM3*B12-TM1*B11                                         SWR16300
      C12 = B14-TM2*B12                                                 SWR16400
      C21 = B23+TM3*B22-TM1*B21                                         SWR16500
      C22 = B24-TM2*B22                                                 SWR16600
      D11 = B33+TM3*B32-TM1*B31                                         SWR16700
      D12 = B34-TM2*B32                                                 SWR16800
      D21 = B43+TM3*B42-TM1*B41                                         SWR16900
      D22 = B44-TM2*B42                                                 SWR17000
      TM4 = D11*D22-D12*D21                                             SWR17100
      V2V1 = D22/TM4                                                    SWR17200
      P2V1 = -D21/TM4                                                   SWR17300
      ZQ11=-(C11*V2V1+C12*P2V1)/W                                       SWR17400
      ZM11=-(C21*V2V1+C22*P2V1)/W                                       SWR17500
      ZQ12 = ZQ11/V2V1                                                  SWR17600
      ZM12 = ZM11/V2V1                                                  SWR17700
      PRINT 335, FREQ,W,A11,A12,A13,A14,B11,B12,B13,B14                 SWR17800
  335 FORMAT (F9.1,F10.1,4E12.3,5X,4E12.3)                              SWR17900
      PRINT 340, A21,A22,A23,A24,B21,B22,B23,B24,A31,A32,A33,A34,B31,   SWR18000
     1 B32,B33,B34,A41,A42,A43,A44,B41,B42,B43,B44                      SWR18100
  340 FORMAT (19X,4E12.3,5X,4E12.3)                                     SWR18200
      PRINT 370, V2V1,P2V1,ZM11,ZQ11,ZM12,ZQ12                          SWR18300
  370 FORMAT (*0  V2/V1 = *,E10.3,*  PSI2/V1 = *,E10.3,*  ZM11 = *,     SWR18400
     1 E10.3,*  ZQ11 = *,E10.3,*  ZM12 = *,E10.3,*  ZQ12 = *,E10.3///)  SWR18500
   45 IF (FREQ-FN(I))35,40,40                                           SWR18600
   35 FREQ = FREQ+FDX(I)                                                SWR18700
```

```
      GO TO 1000                                                        SWR18800
   40 CONTINUE                                                          SWR18900
      GO TO 2000                                                        SWR19000
   15 PRINT 350, W                                                      SWR19100
  350 FORMAT (1H ,3X,E10.3,4X,25HNEAR OR ABOVE SINGULARITY)             SWR19200
      GO TO 45                                                          SWR19300
      END
```

COMPUTATIONS LABORATORY — SOUTHWEST RESEARCH INSTITUTE

PROBLEM: EXAMPLE KEYPUNCH FORM — PAGE OF

PROGRAMMER: CONE — DATE

FORTRAN STATEMENT

Columns 1–10	Columns 11–20	Columns 21–30	Columns 31–40 and beyond
			N for $[f]_i$, $[\Delta f]_i$, $[f]_n$ (FΦRMAT I5)
3			
			a, b, α, AND h (FΦRMAT 4F10.0)
5.0	2.5	15.0	0.005
			ν, E, AND ρ (FORMAT F10.0, 2E10.2)
0.3	3.00+07	7.35-04	
			W, I, AND δ (FΦRMAT 3F10.0)
32.8	0.519	1.08	
			$[f]_i$, $[\Delta f]_i$, $[f]_n$ (FΦRMAT 3F10.0)
20.0	10.0	30.0	
40.0	20.0	100.0	
200.0	100.0	300.0	

INPUT DATA DESCRIPTION (CYLINDER)

CARD NO.	FORTRAN SYMBOL	VARIABLE NAME	UNITS	DEFINITION
1	N	n		Number of frequency sets.
2	SA	a	in.	Radius of cylindrical shell.
	SL	l	in.	Length of cylindrical shell.
	H	h	in.	Wall thickness of cylindrical shell.
3	ENU	ν		Poisson's ratio.
	E	E	psi	Young's modulus.
	RHO	ρ	lb-sec^2/in^4	Mass density.
4	WT	W_t	lb.	Weight of attached mass.
	AI	I	lb-in-sec^2	Moment of inertia of supported mass.
	DEL	δ	in.	Offset of center of supported mass.
5	F_i	f_i	cps	Initial frequency.
	FDX_i	Δf_i	cps	Frequency increment.
	FN_i	f_n	cps	Final frequency.

PROGRAM OUTPUT

Printed Output

1. All input data except I and δ.

2. Frequency f in cps and rad/sec.

3. Characteristic transfer matrix $[\alpha_{ij}]$ and transfer matrix $[\beta_{ij}]$.

4. Translational and rotational velocity ratios $(\dot{V}_2/\dot{V}_1)$ and $(\dot{\Psi}_2/\dot{V}_1)$.

5. Force input and moment input pseudo impedances ZQ11 and ZM11.

6. Force transfer and moment transfer pseudo impedances ZQ12 and ZM12.

7. If $\Omega > 0.99$, an error message will be printed and the program will continue.

PROGRAM NOTES
(CYLINDER)

Subprogram Used

In addition to the main program, the following subroutine subprogram was used.

1. MATINV, computes the inverse of a real matrix.

```
C       PROGRAM CONEIMP
C       PROJECT  0 2 - 2 0 3 4
C       CDC 3600 FORTRAN
        DIMENSION  Y(4),F(4)
        DIMENSION  FRQ(20),FRQX(20),FRQN(20)
        DIMENSION V(4),U(4),BM(4),Q(4)
        DATA (PI=3.14159265),(C1=386.0),(C2=1.74532925E-02),(ERR=1.E-5)
  2000 READ 200, N
   200 FORMAT ( I15 )
        IF (EOF,60)80,85
    80 STOP
C ***  GEOMETRIC PARAMETERS
    85 READ 205, A,SB,ALPHA,H
   205 FORMAT ( 4F10.0 )
C ***  MATERIAL PARAMETERS
        READ 210,ENU,E,RHO
   210 FORMAT ( F10.0,2E10.2)
C ***  RIGID MASS
        READ 215, WT,AI,DEL
   215 FORMAT ( 3F10.0 )
        BMS = WT/C1
        ALFR = C2*ALPHA
        TAN = DSN/DCN
        DCN = COSF(ALFR)
        DSN = SINF(ALFR)
        G = E/(2.0*(1.0+ENU))
        W0 = SQRTF(E/RHO)/A
        GAM = SB/A
        WS = W0*DCN
        FS = WS/(2.0*PI)
C ***  FREQUENCY RANGE
        READ 220, (FRQ(I),FRQX(I),FRQN(I),I=1,N)
   220 FORMAT ( 3F10.0)
        PRINT 300
   300 FORMAT (1H1, 6X,51HCONICAL SHELL LATERAL IMPEDANCE PROGRAM - D.D.
      1KANA//66H THIS PROGRAM CALCULATES (4X4) TRANSMISSION MATRICES BETA
      2(I,J) AND/62H ALPHA(I,J) FOR CONICAL SHELLS UNDER LATERAL EXCITATI
      3ONS, ALSO/66H CALCULATES INPUT AND TRANSFER PSEUDO IMPEDANCES WHEN
      4 AN ARBITRARY/44H MASS M IS ATTACHED TO THE OUTPUT TERMINAL 2)
        PRINT 305, ALPHA,E,A,ENU,SB,RHO,H,BMS
   305 FORMAT (1H0,10X,20HGEOMETRIC PARAMETERS,25X,19HMATERIAL PARAMETERS
      1/26H SEMIVERTEX ANGLE ALPHA = ,F7.3, 8H DEGREES,6X,20HYOUNGS MODUL
      2US   E = ,E10.3, 4H PSI/26H MAJOR BASE RADIUS     A = ,F7.3,7H INCHE
      3S,7X,20HPOISSONS RATIO NU = ,E10.3/26H MINOR BASE RADIUS     B = ,
      4F7.3, 7H INCHES,7X,20HMASS DENSITY  RHO = ,E10.3,17H LB(SEC)**2/IN
      5**4/10H THICKNESS,12X, 4HH = ,F7.3, 7H INCHES,7X, 4HMASS,12X, 4HM
      6= ,E10.3,14H LB(SEC)**2/IN)
        PRINT 320
   320 FORMAT (1H0,34X,17HFREQUENCY ( CPS ))
        PRINT 325, (FRQ(I),FRQX(I),FRQN(I),I=1,N)
   325 FORMAT (30X,F8.1,2H (,F6.1,2H ),F8.1)
        PRINT 310, FS,WS
   310 FORMAT (1H0,23X,33HFREQUENCY SINGULARITY -      FS = ,F8.1/48X,
      1 9HOMEGAS = ,F8.1)
        PRINT 330
   330 FORMAT (*0   FREQ*,5X,*OMEGA*,14X,*((ALPHA(I,J),J=1,4),I=1,4)*,
      1  27X,*((BETA(I,J),J=1,4),I=1,4)*)
        DO 40 I=1,N
        FREQ = FRQ(I)
  1000 W = 2.0*PI*FREQ
        WSQ = W*W
        OMEGA = W/W0
```

```
      OSQ = OMEGA*OMEGA
      DX = (1.0-SB/A)/100.0
      V(3) = BM(2) = Q(1) = 1.0
      V(1) = V(2) = V(4) = 0.
      U(3) = -(DSN*DCN)/(1.0-OSQ*GAM*GAM)
      U(4) = ((DCN*DCN-OSQ*GAM*GAM)*A*GAM)/(1.0-OSQ*GAM*GAM)
      U(2) = -((ENU*DSN)/(PI*E*H*A*GAM))/(1.0-OSQ*GAM*GAM)
      U(1) = 0.
      BM(1) = BM(3) = BM(4) = 0.
      Q(2) = Q(3) = Q(4) = 0.
      IF (OMEGA.GE.DCN)15,10
   15 PRINT 350, FREQ,W
  350 FORMAT (1H ,2F10.1,4X,25HNEAR OR ABOVE SINGULARITY)
      GO TO 55
   10 CONTINUE
      DO 45 J=1,4
      X = GAM
      Y(1) = V(J)
      Y(2) = U(J)
      Y(3) = BM(J)
      Y(4) = Q(J)
      WCAP = -(Y(1)+Y(2)*TAN+((ENU*Y(3))/(PI*E*H*A*DCN*X)))/(1.0-
     1  ((OSQ*X*X)/(DCN*DCN)))
      K = 0
   20 WCAP = -(Y(1)+Y(2)*TAN+((ENU*Y(3))/(PI*E*H*A*DCN*X)))/(1.0-
     1  ((OSQ*X*X)/(DCN*DCN)))
      F(1) = (Y(1)*DSN+(Y(2)/DCN)+(Y(4)/(PI*G*H))+((TAN*Y(3))/(PI*G*H*
     1  A*X)))/(X*DSN)
      F(2) = ((Y(3)/(PI*E*H*A*X*X))-((ENU*OSQ*X*WCAP)/DCN))/DSN
      F(3) = ((PI*E*H*A*OSQ*X*X)/DSN)*(WCAP*TAN-Y(2))-
     1  Y(4)*A*(DCN/DSN)
      F(4) = PI*E*H*OSQ*(X/DSN)*(WCAP-Y(1)+Y(2)*TAN)
      S = RKLDEQ (4,Y,F,X,DX,K)
      IF (S-1.0)25,20,30
   25 STOP
   30 CONTINUE
      IF (X-1.0)20,50,50
   50 CONTINUE
      GO TO (70,72,73,75)J
   70 B11 = Y(4) $ B41 = (Y(2)-WCAP*TAN)/(A*X) $ B31 = Y(1) $ B21 = Y(3)
      GO TO 45
   72 B12 = Y(4) $ B42 = (Y(2)-WCAP*TAN)/(A*X) $ B32 = Y(1) $ B22 = Y(3)
      GO TO 45
   73 B13 = Y(4) $ B43 = (Y(2)-WCAP*TAN)/(A*X) $ B33 = Y(1) $ B23 = Y(3)
      GO TO 45
   75 B14 = Y(4) $ B44 = (Y(2)-WCAP*TAN)/(A*X) $ B34 = Y(1) $ B24 = Y(3)
   45 CONTINUE
      A11 = B11 $ A12 = B12 $ A21 = B21 $ A22 = B22
      A31 = W*B31 $ A41 = W*B41 $ A32 = W*B32 $ A42 = W*B42
      A13 = -B13/W $ A23 = -B23/W $ A14 = -B14/W $ A24 = -B24/W
      A33 = B33 $ A34 = B34 $ A43 = B43 $ A44 = B44
      TM1 = BMS*WSQ
      TM2 = AI*WSQ
      TM3 = TM1*DEL
      C11 = B13+TM3*B12-TM1*B11
      C12 = B14-TM2*B12
      C21 = B23+TM3*B22-TM1*B21
      C22 = B24-TM2*B22
      D11 = B33+TM3*B32-TM1*B31
      D12 = B34-TM2*B32
      D21 = B43+TM3*B42-TM1*B41
      D22 = B44-TM2*B42
```

```
      TM4 = D11*D22-D12*D21                                           SWR12500
      V2V1 = D22/TM4                                                  SWR12600
      P2V1 = -D21/TM4                                                 SWR12700
      ZQ11=-(C11*V2V1+C12*P2V1)/W                                     SWR12800
      ZM11=-(C21*V2V1+C22*P2V1)/W                                     SWR12900
      ZQ12 = ZQ11/V2V1                                                SWR13000
      ZM12 = ZM11/V2V1                                                SWR13100
      PRINT 335, FREQ,W,A11,A12,A13,A14,B11,B12,B13,B14               SWR13200
  335 FORMAT (F9.1,F10.1,4E12.3,5X,4E12.3)                            SWR13300
      PRINT 340, A21,A22,A23,A24,B21,B22,B23,B24,A31,A32,A33,A34,B31, SWR13400
     1 B32,B33,B34,A41,A42,A43,A44,B41,B42,B43,B44                    SWR13500
  340 FORMAT (19X,4E12.3,5X,4E12.3)                                   SWR13600
      PRINT 370, V2V1,P2V1,ZM11,ZQ11,ZM12,ZQ12                        SWR13700
  370 FORMAT (*0   V2/V1 = *,E10.3,*   PSI2/V1 = *,E10.3,*   ZM11 = *, SWR13800
     1 E10.3,*   ZQ11 = *,E10.3,*   ZM12 = *,E10.3,*   ZQ12 = *,E10.3///) SWR13900
   55 IF (FREQ-FRQN(I))35,40,40                                       SWR14000
   35 FREQ = FREQ+FROX(I)                                             SWR14100
      GO TO 1000                                                      SWR14200
   40 CONTINUE                                                        SWR14300
      GO TO 2000                                                      SWR14400
      END                                                             SWR14500
```

COMPUTATIONS LABORATORY — SOUTHWEST RESEARCH INSTITUTE

PROBLEM: EXAMPLE KEYPUNCH FORM | PAGE OF

PROGRAMMER: CYLINDER | DATE

FORTRAN STATEMENT

Columns 1–10	Columns 11–20	Columns 21–30	Comment
			N for $[f]_i$, $[\Delta f]_i$, $[f]_n$ (FØRMAT I5)
3			
			a, ℓ, AND h (FØRMAT 3F10.0)
5.0	15.0	0.005	
			ν, E, AND ρ (FØRMAT F10.0, 2E10.2)
0.3	3.00+07	7.35-04	
			W, I^*, AND δ (FØRMAT 3F10.0)
32.8	0.65	0.56	
			$[f]_i$, $[\Delta f]_i$, $[f]_n$ (FØRMAT 3F10.0)
20.0	10.0	30.0	
40.0	20.0	100.0	
200.0	100.0	300.0	